Glodny, J., Gräfe, K., Echtler, H., Rosenau, M. (2008): Mesozoic to Quaternary continental margin dynamics in South-Central Chile (36°-42°S): the apatite and zircon fission track persperctive. - International Journal of Earth Sciences, 97, 6, 1271-1291

DOI: 10.1007/s00531-007-0203-1.

Mesozoic to Quaternary continental margin dynamics in South-Central Chile (36°-42°S): the apatite and zircon fission track perspective

Johannes Glodny*, Kirsten Gräfe, Helmut Echtler, Matthias Rosenau

GeoForschungsZentrum Potsdam, Telegrafenberg C2, 14473 Potsdam, Germany

* Corresponding author.
email: glodnyj@gfz-potsdam.de; phone: ++49 331 2881375; fax: ++49 331 2881370

Final Draft

International Journal of Earth Sciences (Geologische Rundschau)
doi 10.1007/s00531-007-0203-1

Abstract

Zircon and apatite fission track data provide constraints on the exhumation history, fault activity, and thermal evolution of the South-Central Chilean active continental margin (36°S-42°S), which we use to assess the tectonic and geomorphic response of the margin to the Andean subduction regime. Several domains with different exhumation histories are identified. The Coastal Cordillera is characterized by uniform and coherent exhumation between Late Triassic (~200 Ma) and late Miocene times, with surprisingly slow average rates of 0.03-0.04 mm/a. Thermal anomalies, related to Late Cretaceous and early Miocene magmatism, have regionally modified fission track age patterns. The Upper Cretaceous thermal overprint is of previously unrecognized significance and extent in the Coastal Cordillera south of 39°S. With the exception of a local but distinct Pliocene to Recent exhumation period in the high-relief Cordillera Nahuelbuta segment between 37°S and 38°S, Cenozoic overall exhumation in the Coastal Cordillera was very slow. The sedimentary record shows that uplift and subsidence here was episodic, with low amplitudes and durations. This rules out large-scale, long-term, Cenozoic accretion, trench-parallel tilting, and tectonic erosion processes in the forearc. The Main Andean Cordillera shows markedly greater long-term exhumation rates than the Coastal Cordillera and, at ~39°S, a steep exhumation gradient. To the south, long-term average Pliocene to Recent exhumation rates of ~1 to ~2 mm/a in the Liquiñe area (39°45'S) are almost an order of magnitude more rapid than average Paleogene to Recent exhumation near Lonquimay (38°30'S) and farther north. While no imprint of the intra-arc Liquiñe-Ofqui Fault Zone on the exhumation pattern is evident, long-term exhumation rates decrease from the crest of the Andes towards the western foothills. Exhumation gradients correlate with climatic gradients, suggesting a causal link to the variable intensity of late Miocene to Pleistocene glacial erosion.

Keywords: Exhumation; erosion; fission track analysis; active continental margin; Chile

Introduction

Active continental margins are dynamic systems and the sites of intense mass transfer. Subduction carries fluids, sediments, oceanic crust, and offscraped continental crust toward the Earth's interior, and may cause accretion and magmatic activity. These processes lead to forearc deformation, faulting, mountain building, and ultimately to continental growth and -destruction. In addition, all continental margins also experience erosion, which is controlled by climate, tectonic uplift, and the development of morphology (Burbank 2002; Bonnet & Crave 2003). Erosion is a mechanism that enables exhumation and, more generally, vertical movements of rocks within the crust (Ring et al. 1999, Willett et al. 2003). Thus, for a full understanding of margin dynamics, information on the timing and kinematics of deformation from the rock record has to be linked with quantitative constraints on exhumation histories of individual geologic units within an active margin system.

Fission track analysis yields age information on low-temperature increments of the cooling history of rocks. Given the thermal history of the upper crust is well constrained, fission track ages may provide quantitative estimates on erosional and tectonic exhumation, on tectonic movements at fault zones, and on the thermal evolution of sedimentary basins (Gallagher et al. 1998 and references therein). On cooling, zircon starts to partially preserve fission tracks at temperatures below ~350°-300°C, and quantitatively retains fission track information for prolonged periods at and below ~250-200°C (e.g., Brandon et al. 1998; Tagami et al. 1998; Bernet et al. 2002, Rahn et al. 2004). Zircon fission track retentivity is generally higher for zircon with low amounts of accumulated radiation damage (Rahn et al. 2004). For apatite, this temperature interval, characterized by transient and partial preservation of fission tracks with progressive track fading and termed 'partial annealing zone' (PAZ, cf. Wagner 1979) is between >110 and 60°C (Green et al. 1989; see review in Reiners and Brandon 2006). A combination of zircon and apatite fission track thermochronology thus potentially constrains cooling histories at temperatures between ~300°C and 60°C, which converts, assuming the typical geothermal gradient of the continents, to a record of exhumation from ~10 to 2 km depths.

The active continental margin of South-Central Chile is a particularly well-suited area to study long-term margin evolution and mass transfer patterns. Active margin evolution here has proceeded since the Pennsylvanian, without complications by terrane transport or terrane accretion (cf. Glodny et al. 2006). The study area includes the transition between the high Central Andes and the topographically much lower and narrower Patagonian Andes, and also shows a well-developed forearc high (the Coastal Cordillera), with a major depression (the Longitudinal Valley) in between the Andes and the Coastal Cordillera (see Fig. 1).

The present fission-track reconnaissance study in the margin segment between 36°S and 42°S addresses several key topics of current interest, both in general terms of margin dynamics, and in regional Andean geology.

First, the active margin of northern and central Chile is known as a prime example of subduction erosion, i.e., of continental mass removal from the forearc region into the mantle via a subduction channel, a process that proceeded since the Mesozoic (e.g., Rutland 1971, Von Huene and Ranero 2003). In contrast, for the South-Central Chilean margin, Bangs and Cande (1997) proposed that this margin segment alternated between subduction accretion and tectonic erosion in Pliocene to Holocene times. In comparable forearc settings, exhumation histories of forearc highs were constrained by fission track data, and rock uplift has been attributed to accretion processes (Dumitru 1989, Brandon et al. 1998, Kamp 1999). In South-Central Chile, zircon fission track data constrain, in combination with isotopic data on deformation, the late stages of rapid paleo-exhumation related to basal accretion in the Late Triassic (40°S; Glodny et al. 2005). By studying the thermal and exhumation history of the Coastal Cordillera forearc high we aim at the identification of responses of the forearc region to possible episodes of subduction erosion, accretion, or other forearc-modifying processes.

Second, the South-Central Chilean margin segment between 36°S and 42°S includes marked climatic gradients, with southward-increasing annual precipitation and a maximum annual precipitation on the western flank of the Andean Main Cordillera (New et al. 1999; 2002). During Pliocene to Holocene cool climate episodes, the Andean Main Cordillera south of about 40°S was heavily glaciated and shows much more pronounced glacial erosion than farther north, where only intermittent alpine-type valley glaciers were formed (Rabassa and Clapperton 1990, Rosenau 2004). Fission track data allow the study of correlations between modern precipitation, prolonged glaciation, and long-term erosion rates (Willett 1999, Spotila et al 2004), with implications for crustal dynamics, rock uplift, and deformation. Spatially and temporally varying climatic conditions and glaciation histories along the Andes should be reflected in exhumation rate variations. In particular, fission track data from the studied area should enable the constraint of long-term (Pliocene to Holocene) glacial erosion efficiency (near the Andean continental divide south of 40°S) in comparison to both the efficiency of mixed glacial-and fluvial erosion at lower precipitation conditions farther north, as well as predominantly fluvial erosion in the Andean foothills.

Third, fission track studies revealed that in the Main Andean Cordillera south of 41°S, exhumation is concentrated along a prominent, more than 1000 km long intra-arc, trench parallel fault, the Liquiñe-Ofqui Fault Zone (LOFZ) (Thomson 2002, Adriasola et al. 2006). For the fault segment south of 43°S, Thomson (2002) found that the LOFZ defines crustal segments within

the Andean Cordillera with differential exhumation histories, and that the fault zone is associated with a localized heat flow anomaly. We investigated in detail a profile across the LOFZ fault trace, to constrain the impact of the fault zone on Andean morphogenesis north of 41°S, and to distinguish possible LOFZ-associated tectonic and thermal controls on fission track signatures in the studied region from erosion-related signatures.

The fission track study in this paper comprises 52 new zircon and apatite fission track ages, covering all major currently eroding morphotectonic units in the area. The results reveal an unexpected long-term stability for the forearc high (Coastal Cordillera) with only very slow long-term average exhumation since the Mesozoic, which contrasts with differential, partly rapid Neogene and recent exhumation within the Main Andean Cordillera.

South-Central Chile: morphotectonic units and geological overview

On a transect from W to E, the South-Central Chilean active margin is represented by four major trench-parallel geomorphologic units (Fig. 1). The continental shelf, reaching widths between 50 and 100 km, is associated with a steep slope towards the deep sea trench in the west and locally with narrow coastal plains in the east. The Coastal Cordillera in most areas emerges directly from the shoreline. Its crest is located at a distance of about 130 km from the trench, and reaches altitudes of up to 1500 m in the Cordillera Nahuelbuta at 38°S. However, average maximum elevation is well below 1000 m. Farther east, the Longitudinal Valley constitutes a sediment depository since late Oligocene-early Miocene times (Muñoz et al. 2000; Jordan et al. 2001). In the Andean Main Cordillera the study area consists of a ~200 km wide and on average less than 1200 m high mountain belt. The top of fluvially and glacially dissected basement reaches maximum elevations of ~2000 m. The magmatic arc, at a distance of ~250 km from the trench, generates individual volcanoes on top of Andean basement.

As to the geological situation, the oceanic Nazca plate and the South American continent currently converge at about 66 mm/a (Angermann et al. 1999). Quaternary to recent frontal accretion has formed a small, 20-30 km wide frontal-accretionary wedge on the lower parts of the continental slope (Rauch 2005). However, the upper slope and the entire shelf area are underlain by continental basement (Bangs and Cande 1997), regionally with Upper Cretaceous and Cenozoic sediments on top (Mordojovich 1981). The igneous and metamorphic basement of today's forearc region was assembled in late Carboniferous to Triassic times, in an active margin setting. Magmatic arc granitoids of this paleomargin crystallized in late Carboniferous to early Permian times (305-285 Ma, Hervé et al. 1988; Martin et al. 1999; Lucassen et al. 2004). North

of ~38°S, these granitoids are located in the Coastal Cordillera, while farther south, at ~40°S, they constitute the western flank of the Main Cordillera (Fig. 1). The associated metamorphic basement represents a composite, regionally long-lived accretionary wedge (Hervé et al. 1988; Glodny et al. 2005) and has been subdivided into a 'Western Series' and an 'Eastern Series' (Aguirre et al. 1972), based on lithological characteristics, structural inventory and metamorphic signature.

The Western Series is composed of basally accreted material, passively uplifted by continuing basal accretion and exhumed by erosion (Glodny et al. 2005). Lithologically, it consists of strongly deformed metaturbiditic rocks with major tectonic intercalations of oceanic-plate-derived metabasites, and shows a distinct high-pressure/low-temperature, greenschist- to blueschist facies metamorphic imprint. Isotopic ages for the high-pressure metamorphism decrease from N to S. North of 38°S, peak metamorphic ages are around 300 Ma (Willner et al. 2005; Glodny et al., unpublished data). For the coastal area at ~38°S, metamorphism at ~290 Ma was followed by exhumation to upper crustal depths at ~250 Ma (Rb-Sr mineral data, Glodny et al. 2002). In the Valdivia area, 40°S, the rocks of today's surface level were metamorphosed (8-9 kbar, 420°C) at 250 Ma, and reached upper crustal depths of between 5.5 and 11 km in Late Triassic time (~200 Ma, Glodny et al. 2005). South of 41°S, metamorphic ages are around 230 Ma (Rb-Sr mineral isochrons, Glodny et al. 2002), identical to minimum K-Ar and Ar-Ar mineral ages (Duhart et al. 2001).

In contrast, the Eastern Series consists of folded metaturbidites without any metabasite intercalations and shows a high-temperature/low pressure metamorphic overprint, spatially related to the intrusive late Paleozoic arc granitoids. Metamorphic grade varies between sub-greenschist facies and amphibolite facies. All available isotopic ages for peak metamorphism and late increments of deformation cluster between 300 and 270 Ma in the study area (Rosenau 2004; Lucassen et al. 2004, and references therein). Based on petrological, structural, and age characteristics, the Eastern Series is interpreted as resulting from subduction-related deformation of former passive margin sediments, followed by intrusion of arc granitoids (Hervé et al. 1988; Willner et al. 2000, Willner 2005, Glodny et al. 2006). Exhumation of regional Eastern Series rocks, together with arc granitoids, apparently was nearly completed in the Triassic as suggested by locally overlying unmetamorphosed Triassic sediments (Charrier 1979; SERNAGEOMIN 2003) (Fig. 1).

At about 38°S, the paleoforearc basement is dissected by the Lanalhue Fault Zone, which in its late stages was a major, sinistral, NW-SE striking transverse fault. This fault experienced its last activation in Early Permian times at 280 to 270 Ma (Collao et al. 2003). North of the Lanalhue Fault trace, late Paleozoic magmatic arc granitoids are offset nearly 100 km closer to the present

trench than farther south. The width of the Western Series is correspondingly reduced, from nearly 200 km, between the Longitudinal Valley and the continental slope south of the fault, to only ~100 km, below the continental shelf, north of the fault (Fig. 1). Fault evolution has been interpreted to relate to an Early Permian period of subduction erosion north of 38°S, contrasting with ongoing accretion farther south. Already in Permian times, exhumation of the fault segment at 38°10'S, 73°00'W (Coastal Cordillera) to upper crustal depths of less than 3-4 km was accomplished (fluid inclusion data, Collao et al. 2003).

The Andean Main Cordillera of the study area mainly consists of a partially eroded, Late Jurassic to Miocene magmatic arc (the North Patagonian Batholith, NPB, cf. Mpodozis and Ramos 1989). Miocene intrusive rocks appear to dominate the central parts of the NPB, close to the Quaternary magmatic arc, whereas Cretaceous granitoids prevail farther W and E. Al-in-hornblende barometry indicates that a gradient of exhumation depths exists within the NPB, with considerably deeper levels exposed south of ~40°S than north of 39°S, related to late Miocene to recent exhumation (Seifert et al. 2005). North of 39°S, the NPB is largely covered by late Oligocene to recent sedimentary, volcanosedimentary, and volcanic rocks, volumetrically mainly belonging to the Cura-Mallín Formation (Suárez & Emparan 1995, and references therein). Along the Argentine border between 39° and 38°S, Jurassic sedimentary rocks outcrop as well (Emparan et al. 1992; SERNAGEOMIN 2003), forming the western flank of the Neuquén basin.
A main tectonic feature of the Main Cordillera in the Patagonian Andes is the Liquiñe-Ofqui Fault Zone (LOFZ), a trench-parallel, intra-arc strike-slip zone, more than 1000 km long between ~37°S and ~47°S (Hervé 1976; Cembrano et al. 1996, Rosenau et al. 2006). While for the southern part of the fault a dextral, mildly transpressive neotectonic kinematic regime has been inferred (Cembrano et al. 2002; Thomson 2002), the northernmost part (37°-38°S) grades into an active transtensional fault system (Potent 2003; Melnick et al. 2006a). The segment between 38° and 42°S is a complex, plane strain, brittle fault system that has accommodated more than 80 km of dextral shear since the Pliocene, with northward transposition of the forearc (Rosenau 2004, Rosenau et al. 2006). The LOFZ appears to be linked to a zone of magmatic weakening of the crust, as suggested by the alignment of the strike with Pliocene to recent volcanic centers and edifices along nearly the entire length of the fault zone.

Fission track thermochronology

In this paper, a total of 32 apatite and 20 zircon fission track ages are presented. Sampling was done mainly on a regional basis, roughly along two north-south, trench-parallel transects, one along the Coastal Cordillera, the other one in the western flank of the Andes (Fig. 1). Sampling covered different lithologies and geologic units, both in the Coastal Cordillera and in the Andes, in order to detect possible differential thermal and exhumation histories. Particular attention was paid to both the Lanalhue and the Liquiñe-Ofqui fault zones. Fission track sample profiles have been collected across both faults, in the Cañete-Lumaco area (Coastal Cordillera) and near the town of Liquiñe (Andes), respectively (Fig. 2). Near Liquiñe we also sampled a vertical profile covering ~1400 m difference in altitude.

Analytical procedures

Apatite and zircon were separated from 1-5 kg of rock by crushing, followed by Wilfley table heavy mineral enrichment and magnetic separation (Frantz isodynamic separator). Heavy liquids were used to produce mineral concentrates. Apatite samples were mounted, polished, and etched in 21°C 5.5 mol nitric acid for 20 seconds. Following irradiation, external detector micas were etched in 21°C 40% HF for 45 minutes. Spontaneous fission tracks in zircon were revealed by etching polished grains, mounted in FEP Teflon^{TM}, with an eutectic mixture of KOH and NaOH at 230°C for 20 to 60 h. Mica external detectors were treated the same way as for the apatites. All samples were analyzed using the external detector method. Irradiation of samples, together with muscovite external detectors and dosimeter glass, was performed at the Radiation Center of Oregon State University, USA. Total thermal neutron fluence was aimed at ~$1x10^{15}$ ncm^{-2} for zircon and at ~$9x10^{15}$ ncm^{-2} for apatite samples, respectively, and has been monitored by Corning U-dosed standard glasses (CN-2 for zircon and CN-5 for apatite). Spontaneous and induced fission track densities were determined using a Zeiss Axioplan-2 optical microscope at 1250x magnification at the GFZ Potsdam, equipped with a computer-controlled Kinetek^{TM} microscope stage, a microscope drawing tube, and a digitizing tablet (cf. Dumitru 1993). Zeta values of 143 ± 10 (CN-2 dosimeter glass) for zircon and 354 ± 15 (CN-5) for apatite were obtained by calibration against international zircon and apatite age standards following the recommendations of Hurford (1990). Results of standard measurements are presented in Tab. 1. The zeta value used here for apatite (354 ± 15, CN-5) includes standard data from previous work published by the fission track analyst K. Gräfe (Gräfe et al. 2002). Ages were calculated as central ages (Galbraith & Laslett 1993), which are model ages weighted to account for the difference in precision of the individual crystal ages within a sample, and which allow for non-

Poissonian variation within a population of single-grain ages. A chi-square statistic was used to assess the probability of grains counted in a sample belonging to a single population of ages (Galbraith 1981).The use of central ages also takes possible operator-related overdispersion into account, as overdispersion ($P\chi^2$ <5%) is occasionally observed in analytical data for standards (Tab. 1). For selected suitable apatite samples, track length distributions have been determined by examination of tracks which are oriented near-parallel to the mount surface and fully enclosed in the crystal. Track lengths have been measured after calibration of the microscope system against an object micrometer.

Results

Results of apatite and zircon fission track analysis are presented in Tab. 2 (zircon, Coastal Cordillera), Tab. 3 (apatite, Coastal Cordillera) and Tab. 4 (apatite, Andes). Fig. 2 shows the locations of the fission track ages. Track length distributions are presented in Fig. 4.

Zircon fission track age data from the Coastal Cordillera area show a large spread. While most samples yield ages between 240 and 140 Ma (Triassic-Jurassic), samples from the area near Valdivia (39°45'S) show Cretaceous ages. Particularly, samples from the southern part of the study area are further characterized by significant spread in single grain ages and presence of mixed grain age populations, as evident from chi-square probabilities <5% (Tab. 2).

Completion of a continuous apatite fission track N-S profile for the Coastal Cordillera area proved to be difficult. Out of a multitude of samples collected from the metamorphic rocks of the region, only a few had apatite with sufficient U for dating. In particular, metamorphic apatite from Western Series lithologies is commonly virtually devoid of uranium. However, some results from these rocks have been obtained and can be integrated with the data from granitoids of the Coastal Cordillera north of 38°S. With few exceptions, the apatites from the Coastal Cordillera area yield Upper Cretaceous to Paleocene ages, between 106 and 54 Ma (Tab. 3).

Within the Andes, very young, Plio-Pleistocene ages between 3 and 1 Ma near the main axis of the Cordillera contrast with older, Miocene to Eocene ages of up to 40 Ma further to the west and north (Tab. 4). This trend is apparent from the Cretaceous granitoid rocks, while geologically younger rocks in the northern parts of the study area (Fig. 2) similarly show Miocene to Pliocene ages.

Discussion

Zircon fission track data, Coastal Cordillera

In the Coastal Cordillera and along the coast, the zircon fission track ages from samples of the Carboniferous to Triassic igneous and metamorphic basement do not show any principal geographic break but a vague general trend of younging towards the south.

Zircon fission track ages range consistently between 179 ± 49 and 242 ± 29 Ma (Triassic to Early Jurassic) in all igneous and metamorphic basement units in the northern part of the study area, i.e., the Cordillera Nahuelbuta region (Fig. 2; roughly between 37°S and 38°S). The numerically youngest and oldest ages overlap within error intervals and were determined for samples collected close to the Lanalhue Fault Zone (Fig. 2). Several independent constraints on the regional exhumation history aid interpretation of these results. Both the Nahuelbuta arc granitoids and the host Eastern Series metamorphic rocks appear to have been exhumed and cooled to temperatures below the brittle-ductile transition by the Permian (>264 Ma), as no younger indications for ductile deformation have ever been detected (Lucassen et al. 2004). For the Lanalhue Fault Zone (38°10'S, 73°00'W), paleotemperatures at or slightly below 200°C at ~270 Ma were determined (Glodny et al., unpublished data; Collao et al. 2003). These temperatures are near the lower temperature limit of the zircon fission track partial annealing zone (Brandon et al. 1998; Tagami et al. 1998; Bernet et al. 2002). In the basally accreted Western Series between 37°S and 39°S, rapid exhumation by active basal wedge growth slowed down and waned by the Early Triassic, when mineralized brittle tension gashes formed at an upper crustal level (Tirúa area, tension gashes isotopically dated at ~250 Ma, Glodny et al. 2002). This is in line with the subvolcanic intrusion level, evident from partly porphyric textures and abundance of miarolitic cavities, of a small Triassic leucogranitic intrusion at the Hualpén peninsula near Concepción, located close to the Western Series-Eastern Series contact and dated at 222 ± 2 Ma (Lucassen et al. 2004). Further, Middle to Late Triassic basins filled with non-metamorphic, marine and continental volcanosedimentary successions (e.g., Charrier 1979; Franzese and Spalletti 2001, and references therein) are discordantly overlying the regional Permo-Carboniferous magmatic arc intrusives and associated Eastern Series rocks (Galvarino basin NNW of Temuco, and Santa Juana basin SE of Concepción, Fig. 2), which implies near-surface positions of parts of this basement already in the Triassic. These basins locally contain coarse grained clasts of the regional basement (Charrier 1979; Hervé et al. 1976), indicating fairly rapid local erosion with distinct morphological relief in Middle to Late Triassic times. A zircon fission track age of 210 ± 17 Ma for a sandstone of the Santa Juana basin (Tab. 2, Fig. 2) is indistinguishable within errors from the regional basement ZFT age pattern, suggesting that

the unmetamorphosed Triassic sediments share a common thermal history with the regional basement after sediment deposition.

Together with the above geologic constraints, the zircon fission track ages from the Cordillera Nahuelbuta region indicate that cooling of the now exposed basement units to temperatures below the lower ZFT PAZ limit (~220-200°C for slow cooling; Brandon et al. 1998; Tagami et al. 1998; Bernet et al. 2002) was locally achieved as early as at around 270 Ma, and definitely completed by the Late Triassic, at about 200 Ma. This completion may have been associated with a period of enhanced erosion during formation of the Triassic basins, which were in turn related to extension, magmatism, and continental rifting (Franzese and Spalletti 2001 and references therein). Assuming a 'normal' average geothermal gradient of ~30°C/km, which is consistent with present-day heat flow data of Hamza and Munoz (1996) for the area, exhumation since the Late Triassic should amount to about 7 km. For the area north of 38°S, which has been affected by Triassic rifting, this exhumation estimate may in fact be an overestimation of the total exhumation as extension and rifting has been associated with a period of anomalously high heat flow (Franzese and Spalletti 2001; Belmar et al. 2002). Thus, the ZFT ages in this region probably date the end of this high heat flow episode at paleodepths of consequently less than 7 km.

Despite the contrasting peak metamorphic pressures and temperatures of Western and Eastern Series rocks, no significant difference in ZFT ages between these different lithologies on both sides of the Lanalhue Fault Zone (38°S) is observed, confirming that the last major vertical displacements related to this fault zone are pre-Triassic in age. Further, ZFT ages suggest that basal accretion (and associated rapid exhumation) within the Western Series at around 38°S came to an end in late Permian to Early Triassic times. North of the study area, between 34°30'S and 35°40'S, recent zircon fission track analyses of Coastal Cordillera units have also yielded Triassic ages for both Western and Eastern Series rocks (Willner et al. 2005). It thus appears that the long stretch of the present Coastal Cordillera between about 34°30' and 38°30' S is characterized by a regionally uniform cooling in the Triassic through the ZFT PAZ.

The above regional pattern of ZFT ages north of 38°30'S contrasts with a ZFT age of 135 ± 17 Ma, characterized by a heterogeneous grain age distribution, from an Upper Cretaceous sandstone from Dichato, Pacific coast at 36°34'S (Fig. 2). Obviously, this Cretaceous depocenter preferentially collected detritus from sources with considerably younger ZFT cooling ages than found in the Coastal Cordillera basement, possibly from Early Andean (Jurassic-Cretaceous) magmatic arc rocks.

The basement in the Coastal Cordillera south of ~38°30'S is dominated by Western Series rocks, the early exhumation history of which differs significantly from the forearc segment farther

north. The ages of peak metamorphic conditions in today's surface material show a clear trend of younging towards the south, as outlined above, from ~290 Ma near Tirúa (38°15'S) to ~230 Ma at 40°45'S. Even farther south on the island of Chiloé at 42°S, K-Ar and Ar/Ar muscovite ages of 232 ± 3 and 220 ± 6 Ma have been reported and interpreted as cooling ages (Duhart et al. 2001). Peak metamorphic temperatures of the Western Series exceeded 350°C (Willner et al. 2001; Glodny et al. 2005). ZFT ages can thus be interpreted as cooling ages in these rocks. Using three previously published ZFT ages in combination with Rb/Sr dating and fluid inclusion studies, the 230-200°C paleotemperature level in Western Series rocks, east of Valdivia (39°45'S) and distant from a local intrusive body, has been dated at ~210-185 Ma (Glodny et al. 2005), which is still similar to the above constraints for the Coastal Cordillera N of 38°30'S. However, south of 40°S, ZFT data appear to be significantly younger, in the range between 164 and 140 Ma (Fig. 2). This regional pattern has an extension towards the south. On Chiloé island, a Jurassic ZFT age of 155 ± 10 Ma has been reported from the northern tip of the island (41°48'S; Adriasola 2003). This age is identical within limits of error with the 164 ± 21 Ma age determined for a sample collected only a few km away (Fig. 2). Similar ages of 155 ± 7 and 142 ± 7 Ma were also found in central Chiloé (42°20'S; Thomson and Hervé 2002).

Two possible interpretations of these formally Jurassic ages may be discussed. On one hand, for the Valdivia area (39°45'S) it has been shown that a period of roughly 50-60 Ma was necessary in the actively evolving accretionary complex to cool and exhume basally accreted material from peak metamorphic conditions to the 200°C paleotemperature level (Glodny et al. 2005). Given the fact that south of 40°S, peak metamorphic conditions for currently exposed material were reached 20-30 Ma later than near Valdivia (220-230 Ma vs. 250 Ma near Valdivia), the Jurassic ZFT ages may simply reflect prolonged activity of the accretionary system south of 40°S compared to forearc segments farther north. However, on the other hand, all but one ZFT datasets from the mainland south of 40°S and Chiloé fail the chi-square test ($P\chi^2$ <5%, Tab. 2); the age data thus have no direct geological meaning. Thorough examination of the corresponding heterogeneous grain-age distributions led Thomson and Hervé (2002) to propose an Upper Cretaceous local reheating event as affecting their Chiloé samples. Such a Cretaceous thermal event is also compatible with the more recent detection of several Upper Cretaceous zircon fission track ages in central and southern Chiloé (Adriasola 2003). In fact, detailed examination of the new ZFT data reveals grain-age distributions strikingly similar to those published by Thomson and Hervé (2002). The new ZFT data is characterized by the coexistence of grain ages at or slightly above 200 Ma, with a distinct population of youngest ZFT ages around 100 Ma (Late Cretaceous; Fig. 3). This age value coincides with the age of the

Chaihuín granodiorite in the Valdivia region and some satellite intrusive bodies nearby, the crystallization of which is dated at 91.3 ± 4.9 Ma (U/Pb zircon data, Martin et al. 1999).
Close to the Chaihuín granodiorite, ZFT ages are almost completely reset (samples VAL11, VAL19; ZFT ages of 90 ± 12 Ma and 111 ± 10 Ma, respectively), while zircon from within the intrusive bodies yields ZFT ages of 72 ± 8 to 78 ± 8 Ma (Fig. 2, Tab. 2). This Cretaceous reheating event is evident in the field only from the Upper Cretaceous Chaihuín granodiorite and from sparse granitoid dykes between 39°S and 40°S which are inferred to be Cretaceous in age as well (SERNAGEOMIN 2003), but is obviously of major regional significance. It appears to have affected the entire Coastal Cordillera area south of 39° as well as Chiloé island.
As a consequence, given the regional peculiarity of ZFT ages between ~40°S and 42°20'S with some ZFT ages of around 200 Ma and otherwise partly reset ages, it seems plausible that in this region the 220-200°C paleotemperature and ~7 km paleodepth level were reached in Late Triassic time (~200 Ma), in similarity to the areas farther north. Magmatic activity, as manifested by the Chaihuín granodiorite, must have led to a very significant increase in the upper crustal paleogeothermal gradients in the Coastal Cordillera region south of 39°S in Upper Cretaceous times, in a much more extended region than previously thought. As stated already by Thomson and Hervé (2002), it appears worthwhile to examine the affected area for mineralizations related to hidden Cretaceous intrusions.

Apatite fission track data, Coastal Cordillera

Apatite fission track data for igneous and metamorphic basement units of the Coastal Cordillera region can be subdivided into three distinct groups. North of 39°S, ages are consistently between ~100 and 55 Ma, with no obvious geographic variation or correlation to any regional faults. Close to the Chaihuín granodiorite (39°50'S), all samples show ages between 54 and 70 Ma, both within the granodiorite and in the surrounding schists. South of 40°S, younger AFT ages of 40 and 26 Ma have been found.
Most AFT samples collected between 37°S and 39°S pass the chi-square test, indicating the presence of concordant distributions of grain ages. Coastal Cordillera granitoids north of 38°S yield track length distribution histograms showing mean track lengths <13 µm (Fig. 4a-d) and standard deviations between 1.26 and 1.77 µm, which are related to a significant amount of shortened tracks. Samples 00-31 and 00-32 also show a characteristic negatively skewed distribution (Fig. 4a, b), which is indicative of near-linear slow cooling and prolonged residence within the apatite partial annealing zone (Gleadow et al. 1986; Gallagher et al. 1998). The Upper

Cretaceous to Paleocene AFT ages from both the magmatic and metamorphic rocks north of 39°S therefore suggest slow cooling through the apatite PAZ generally in Upper Cretaceous times, with cooling through the ca. 110°C isotherm possibly considerably earlier than indicated by the numerical fission track age. Clear indications for significant Cenozoic differential exhumation along faults, or for Cenozoic local thermal anomalies, are not observed. Subduction of oceanic crust was continuously going on underneath the Coastal Cordillera at least since the Jurassic (Mpodozis and Ramos 1989), suggesting a more or less 'steady state' thermal situation of the crust through Cretaceous and Cenozoic times. This implies absence of distinct pulses of conductive cooling, and suggests that cooling since the Cretaceous was dominantly exhumation-related, in a thermal regime similar to the present-day situation. Data on the present-day heat flow in the region (Hamza and Muñoz 1996) suggest a fairly 'normal' geothermal gradient in the Coastal Cordillera of the entire study area. Assuming an average value of 30°C/km, total exhumation since the Upper Cretaceous is ≤3 km. For the area between 37°S and 39°S, this is in line with preservation of Triassic sediments on top of the Permo-Carboniferous igneous basement (Fig. 2). Within a regional context, Cretaceous AFT ages between 113 and 80 Ma, i.e., on average only slightly older than in our sampling area, also characterize Coastal Cordillera basement units farther north, between 35°30'S and 34°S (Willner et al. 2005).

In the Valdivia area, the thermal anomaly imposed by the Upper Cretaceous intrusion of the Chaihuín granodiorite has set AFT ages. In that area, AFT ages between 69.7 ± 6.2 and 53.6 ± 5.4 Ma have been obtained for samples with zircon FT ages between 90 and 76 Ma (Fig. 2). After intrusion of the granodiorite at 91.3 ± 4.9 Ma (Martin et al. 1999), it thus took ca. 20-30 Ma (since AFT ages are minimum ages) to cool to about 110°C. The crystallization depth of the exposed granodiorite was at 2-3 km, as constrained by Al-in hornblende data (Seifert et al. 2005) and by the presence of subvolcanic lithologies. Crustal cooling after the regionally important magmatic event (see above) may well have lasted for a prolonged period of time. We interpret the AFT ages as dating thermal relaxation, possibly aided by concurrent exhumation, in Upper Cretaceous to Paleocene times within the uppermost 3 km of the crust.

To get a more detailed insight into the thermal history of the Coastal Cordillera segment between 37°15'S and 40°S, we modeled time-temperature histories. Inverse modeling has been performed using the AFTSolve software, v. 1.3.0 (Ketcham et al. 2000; Ketcham and Donelick 2003) with default settings that take into account that kinetic data for the apatites are not available. Fission track age data and track length distributions were modeled for four samples from the Cordillera Nahuelbuta segment of the Coastal Cordillera (37°15'S-37°45'S; samples 00-83, 00-77, 00-31, 00-32, Tab. 3) and for one sample (VAL14) from the Chaihuín granodiorite, Valdivia area (~39°50'S). Results are presented in Fig. 5. Although the results can only be used

as qualitative hints, it appears that the time-temperature histories for the high-relief Cordillera Nahuelbuta segment are all similar at least for the Cenozoic. They they include a signal from a distinct Plio-Pleistocene 'final' cooling episode, probably corresponding to evolution of high relief (peak elevations ~1500 m above sea level) and concomitant erosion in that particular area since the late Miocene (Rehak 2005, Melnick and Echtler 2006a). In contrast to the Cordillera Nahuelbuta area, no such distinct Plio-Pleistocene cooling episode is evident from the available data for the Coastal Cordillera near Valdivia (Fig. 5).

The two AFT samples from south of 40°S (39.7 ± 3.2 Ma and 26.3 ± 2.8 Ma, Fig. 2) are considerably younger than all data collected farther north. The 26.3 Ma AFT age from Ancúd/Chiloé most likely reflects resetting by intense regional Miocene magmatic activity, dated at ~24-20 Ma (Muñoz et al. 2000). This interpretation is corroborated by a 67 ± 11 Ma AFT age for a sample from the northern tip of Chiloé island (Adriasola 2003). This sample was collected only a few km away from our 26 Ma sample, which shows that the Miocene thermal imprint reflects local thermal anomalies instead of a regional cooling pattern. Several Upper Cretaceous AFT ages of between 92 ± 28 and 68 ± 8 Ma from the Coastal Cordillera of northern Chiloé (42°00'S - 42°30'S; Thomson and Hervé 2002; Adriasola 2003), interpreted as reflecting steady cooling (Thomson & Hervé 2002) add to our set of Upper Cretaceous cooling ages from north of 40°S. Therefore, within the regional context of the Coastal Cordillera between 37° and 42°20'S, post-Upper Cretaceous ages appear to be anomalous and defined by local Cenozoic thermal anomalies rather than by exhumation-related cooling.

Coastal Cordillera exhumation history

Considering the new AFT data, it appears that the entire Coastal Cordillera in the study area was exhumed to crustal levels of ≤3 km at ≥70 Ma, i.e., in Upper Cretaceous times. Combining the above geologic and paleogeothermal constraints with ZFT and AFT data for the area between 37°S and 42°S yields a long-term average exhumation rate of ~0.03 mm/a for Late Triassic to Late Cretaceous times all along the studied Coastal Cordillera segment. This average exhumation rate is remarkably low when compared to the world-average continental erosion rate of ~0.05 mm/a (Ring et al. 1999, and references therein). The very slow post-Triassic exhumation is in sharp contrast to the more than one order of magnitude higher average exhumation rates of Western Series rocks during ongoing basal underplating in the Permo-Triassic (Glodny et al. 2005). Therefore, between 200 and 70 Ma today's Coastal Cordillera region most likely has been a low-relief, tectonically stable region.

A similarly very low long-term average exhumation rate of ~0.04 mm/a can be calculated for Late Cretaceous to Recent time from the AFT dataset. However, locally vertical movements occurred in that period, possibly associated with more pronounced erosion. Locally preserved Pliocene-Pleistocene marine sedimentary cover on basement rocks in the Coastal Cordillera suggests uplift of several 100 m, and up to nearly 1000 m in the Cordillera Nahuelbuta since the Pliocene, while Miocene onshore basins point to local subsidence in the late Oligocene-early Miocene. Thus, the actual land surface appears to have been affected by episodic uplift and subsidence in the Cenozoic. However, these processes most likely did not lead to exhumation detectable by the apatite fission track method. Episodic evolution of mountains, such as in the Valdivia vicinity in the early Miocene (cf. le Roux & Elgueta 2000), is only reflected in the apatite fission track dataset for the Plio-Pleistocene emergence of the Cordillera Nahuelbuta as a high-relief area. It did not result in pronounced long-term exhumation elsewhere (Fig. 6). Thus, apart from 'breathing'-like oscillations of mean elevation, possibly correlated with episodic changes between accretion and tectonic erosion (Bangs & Cande 1997), the Andean forearc region appears to be remarkably stable, which rules out any large-scale, long-term basal underplating, accretion, trench-parallel tilting, or tectonic erosion processes in the time interval between the Late Cretaceous and the late Miocene. The Cordillera Nahuelbuta segment (~ 37-38°S) of the Coastal Cordillera experienced a distinct uplift and exhumation episode in Pliocene to Recent time, as is evident from forearc tectonics (Melnick and Echtler 2006a, Melnick et al. 2006b), morphometry (Rehak 2005) and from the apatite fission track data. Regional uplift in Plio-Pleistocene times in the 37°S-38°S forearc segment is further indicated by the emergence of the Arauco peninsula. This peninsula is interpreted as an uplifted part of the former offshore forearc (e.g., Mordojovich 1981) where Plio-Pleistocene marine sediments are presently located several 100 m above sea level.

Apatite fission track data, Andean Main Cordillera

Interpretation of the AFT data from the Andean intra-arc zone in terms of deformation and exhumation poses difficulties due to the magmatism-related fluctuations in the paleogeothermal field. Further, in regions with intense Miocene to recent magmatism, pre-Miocene information may be erased and only the post-magmatic cooling history may be accessible. To distinguish between regional AFT signatures and local thermal perturbations, we combine the AFT data with relevant information on local geology, granitoid intrusion depths, and morphostructural evolution.

At 39°45'S, in the Liquiñe area, sampling was done along a W-E profile to delineate the thermo-kinematic and exhumational evolution of that region. Possible effects related to neotectonic movements along the Liquiñe-Ofqui Fault Zone have been the main target here. Thomson (2002) has shown that in its southern segment, at ~43-46°S, the LOFZ defines crustal blocks with differential exhumation histories and is the locus of a narrow late-Cenozoic high heat flow anomaly. In the Liquiñe area, the LOFZ is located only some 10 km W of the Andean continental divide. On a W-E profile, apatite fission track ages get progressively younger, from 16.4 ± 1.0 Ma in the western Andean foothills, to late-Pliocene ages of around 2-3 Ma near Liquiñe, and Quaternary ages as low as 1.2 ± 0.2 Ma near the continental divide. This trend is independent of local rock types and high-temperature isotopic ages, which span a range from the late Carboniferous to the Miocene (cf. Lara & Moreno 1998). On this W-E profile, there is no distinct evidence for differential exhumation along the LOFZ. In contrast, the map-view age data pattern suggests that the entire area experienced exhumation-related cooling in a pronounced W-E gradient. This was possibly accompanied by faulting between the Andean foothills and Liquiñe, with most recent and rapid cooling near the continental divide, along the Chilean-Argentine border. Observations supportive of this inference include results from a vertical profile collected near Liquiñe consisting of samples LOF10, -12, -13, and -14 (Tab. 4). In this profile, the oldest regional AFT age is observed for the sample collected at the highest altitude (LOF12 at 1720 m; 3.5 ± 0.4 Ma, Tab. 4.), while for samples from lower altitudes unsystematically younger ages down to 2.1 ± 0.3 Ma were found. Sample LOF12 is characterized by an abundance of long tracks (mean track length of 14.48 µm) and a very narrow length distribution (S.D = 1.05 µm; Fig. 4g), indicative of rapid passage through the apatite PAZ (Gleadow et al. 1986; Fitzgerald et al. 1995). For sample LOF10 (2.2 ± 0.4 Ma, Tab. 4, Fig. 4f) only a very limited amount of confined tracks has been found; however, with a mean track length of 13.44 µm, dominance of unannealed, long tracks is evident here as well. Secondly, all AFT data from the area pass the chi-square test, which suggests fairly simple cooling histories consistent with cooling by progressive exhumation. For the Andean foothills sample (LOF131, Tab. 4, Fig. 4h), age and track length distribution indicate a distinct episode of cooling in the Mid Miocene but very minor cooling since. Third, a thermal pulse at ~2 Ma causing a complete reset of ages at this time within the wider Liquiñe region is unlikely as magmatic arc activity is confined to specific volcanic centers, and a magmatically controlled, inhomogeneous thermal field would most probably not result in the observed homogeneous regional age pattern. In addition, there has been no important intra-arc extensional tectonism in Pliocene times in the Liquiñe area and farther south (Thomson 2002; Rosenau 2004). We therefore conclude that erosional unroofing, progressively

intense from W to E, was responsible for the Pliocene-Quaternary cooling and exhumation in the Liquiñe area.

Farther towards the north, Miocene granitoids between 38°45'S and 39°10'S provide AFT ages between 4.2 ±1.2 and 5.7 ± 0.8 Ma (samples WS2, LOF135, LOF132, Tab. 4, Fig. 2). The crystallization ages of these granitoids are most likely close to 11 Ma, as suggested by concordant K-Ar ages for amphibole and biotite (Emparan et al. 1992) for the intrusion from which sample WS2 was collected. The only available AFT length distribution data (sample WS2, Fig. 3k) shows that the majority of tracks are long, which points to fairly rapid cooling through the apatite PAZ by the end of the Miocene. Post-Miocene exhumation in this area must have been considerably less than near Liquiñe.

Near the town of Lonquimay (38°30'S), an Upper Cretaceous (Emparan et al. 1992) granitoid is intrusive into Jurassic volcanosedimentary strata. AFT analysis of two samples yielded ages of 34.3 ± 4.6 and 40.5 ± 6.3 Ma (LOF149, LOF171, Tab. 4). These two concordant ages are in marked contrast to the late Pliocene to Quaternary ages from the Liquiñe area. A length distribution histogram for sample LOF171 shows a broad peak with significantly reduced mean track lengths (M.L. = 12.66 µm, S.D. = 1.65 µm, Fig. 4j) which is considered typical for slowly cooled and slowly exhumed basement (Gleadow et al. 1986). While sample LOF149 passes the chi-square test, suggesting a simple cooling history, a $P\chi^2$ value of 4% for sample LOF171 may indicate a slight disturbance, possibly related to reheating by a magmatic dyke intrusion nearby. We interpret these Paleogene AFT ages as indicating much slower exhumation in this area when compared to the Liquiñe region. Preservation of sub-greenschist facies Jurassic sediments indicates that total exhumation since that time must have been less than ~5 km. This is in line with our observation of a very narrow (~50 m) contact metamorphic aureole in Jurassic limestone around the exposed roof of a Cretaceous intrusion near Cerro Pino Solo (2715 m, Chilean-Argentinian border at 38°30'S).

The results from the two samples from north of 38°10'S do not contrast with the inference of fairly slow late- and post-Miocene exhumation in the north of the study area. The significance of the result from sample LOF145 (3.9 ± 0.7 Ma; Fig. 2, Tab. 4) is unclear due to widespread late Miocene to Pliocene magmatic activity nearby. Sample LOF143, from the roof of a subvolcanic Miocene-age intrusion, shows a late Miocene AFT age of 7.8 ± 0.7 Ma, with a negatively skewed track length distribution (Fig. 4i). This is indicative for slow cooling through the apatite PAZ followed by comparatively slow exhumation.

For the intra-arc zone, conversion of AFT cooling ages into estimates of exhumation rates is not straightforward and is fraught with uncertainties, arising from magmatism-related transient thermal anomalies, generally high heat flow modified by hydrothermal heating and cooling effects, and thermal field distortions due to rapid exhumation and topographic evolution (Stüwe et al. 1994; Mas et al. 2000; Moore and England 2001; Rothstein and Manning 2003). However, background upper crustal geothermal gradients in magmatic arcs rarely exceed 50°C/km. The intra-arc zone of the study area is characterized by a positive heat flow anomaly with respect to adjacent morphotectonic units, with surface heat flow values of around 140 mW/m^2 (Hamza and Muñoz 1996). From combination of this value with thermal conductivity estimates for granitoids (Clauser and Huenges 1995; Seipold 1998), we adopt a background gradient of 40±10°C/km as realistic for the investigated intra-arc domain.

With a value of 110°C as an estimate for AFT retention, the AFT age data from the Liquiñe area (3.0-1.2 Ma) convert into Plio-Pleistocene exhumation rates of between ~1 and ~2 mm/a. The Liquiñe vertical AFT age profile discussed above yields an apparent exhumation rate of ~1 mm/a, which is, despite its considerable uncertainty, consistent with the above range of exhumation rates. In contrast to these inferences from the Liquiñe area, the Paleogene AFT age data from Lonquimay result in long term average exhumation rates of ~0.07 mm/a, or even less if slow-cooling-related track length reduction effects are considered. The AFT age of sample LOF143 (37°23'S; 7.8 ± 0.7 Ma) formally allows calculation of an exhumation rate of 0.3 mm/a since cooling below 110°C. However, this is only a maximum estimate due to the Miocene intrusion age of the studied rock.

It thus appears that there is a transition within the study area from generally slow long-term exhumation north of about 39°S at least since Oligocene times, to very rapid, nearly one order of magnitude faster exhumation in the intra-arc zone south of ~39°S (Fig. 6). This conclusion is generally in line with other observations made both in the study area and in adjacent segments of the Andes. First of all, Seifert et al. (2005) have shown, using Al-in-hornblende geobarometry, that a similar N-S gradient in exhumation rates is obvious from granitoid crystallization depths. For both Mesozoic and Miocene arc granitoids, a southward increase in exhumed crystallization depths has been documented, from around 3 km at 37-38°S (equivalent to exhumation rates ≤0.3 mm/a since the late Miocene) to ≥10 km at 41-42°S (equivalent to exhumation rates of ~1 mm/a since the late Miocene). South of the study area, in the intra-arc zone east of Puerto Montt at ~41°15'S, AFT ages determined by Adriasola (2003) show a trend of younging towards the east, strikingly similar to the results from the Liquiñe area. The oldest AFT age here (24.9 ± 4.7 Ma) was found in the western foothills of the Andes, at the shores of Lago Llanquihue. Further

east, near the LOFZ fault trace and at a distance of ~30 km from the continental divide, AFT ages are between 7.2 ± 2.6 and 3.3 ± 1.2 Ma with a cluster of around 4 Ma. This is interpreted to imply exhumation rates of 1-2 mm/a between 5 and 3 Ma (Adriasola et al. 2002; Adriasola 2003; Adriasola et al. 2006). However, at 41°15'S the lowest AFT ages are found close to the trace of the LOFZ, implying that fault-related processes had an impact on the AFT age pattern, in contrast to the observations in the Liquiñe area (39°45'S). At around 42°S, Pankhurst et al. (1992) derived a Pliocene-Pleistocene exhumation rate of ≥1 mm/a for the area near to and east of the LOFZ, in absence of major crustal shortening or compression.

North of ~39°S, where the AFT ages imply slow exhumation, slow long-term average exhumation is further inferred from the more coherent preservation of the late Oligocene- to Miocene Cura-Mallín formation west of the Andean continental divide (Jordan et al. 2001), and the local preservation of unmetamorphosed Jurassic sediments (SERNAGEOMIN 2003, Kemnitz et al. 2005, and references therein). This transition zone between the higher South-Central and the Patagonian Andes is also marked by only limited orogenic contraction in time and space. Low amounts of Neogene orogenic shortening is restricted in the Lonquimay area to a period between ~13 and 8 Ma and does not contribute to considerable exhumation (Vietor and Echtler 2006). Surprisingly low amounts of total Cenozoic exhumation are further inferred from the Eocene AFT ages of around 50 Ma in Jurassic strata close to the continental divide in the Andes near Termas del Flaco, 35°S (Waite et al. 2005). The inferred slow long-term mean Cenozoic exhumation north of 39°S, and at least up to 35°S, at first sight seems to contrast with the interpretation of AFT data from the Tatara-San Pedro volcanic complex (36°S). Here, Plio-Pleistocene AFT ages have been determined and interpreted, together with $^{40}Ar/^{39}Ar$ ages, as indicating exhumation of up to 0.9 mm/a since late Miocene times (Nelson et al. 1999). However, the corresponding time-integrated rapid erosion in this area may be sustained by very pronounced local relief and considerably higher average surface elevation than between 39°S and 37°S, which may have given rise to a local maximum for glacial erosion in that area. In any case, even at 36°S, Miocene to Oligocene volcanosedimentary rocks are widespread, so that even here total exhumation since the early Miocene did not exceed a few km even here.

The emergent consistent pattern of a highly significant decrease of Miocene to Recent time-integrated exhumation rates from south to north, with the most pronounced gradient at ~39°S, requires further explanation. There is no marked transpression or extension documented in the entire study area (see above), so that such factors are not responsible for the observed exhumation rate gradient. Absence of transpression further rules out major tectonic uplift of the area as a driving force inducing accelerated exhumation in the south. This leaves density changes at depth (Platt & England 1993), or emplacement of weakened crust or magma

beneath the region of erosion (cf. Reiners and Brandon 2006) as possible processes to passively balance out exhumation-related mass removal. Mpodozis & Ramos (1989) were the first to propose that the evolution of the apparent regional exhumation gradient is driven by more effective erosion in the south, i.e., related to climatic effects. In fact, recent annual precipitation shows a steep gradient between 42°S and 37°S within the Cordillera, with more than a factor of two higher precipitation in the south (New et al. 1999; 2002). However, the present day precipitation pattern indicates that the annual average precipitation is highest on the western flank of the Andes (New et al. 2002), i.e., not near the continental divide where AFT-derived exhumation was most rapid. Rapid exhumation close to the continental divide was probably related to mechanism other than fluvial incision. Detailed geomorphic analysis shows that the degree of glacial dissection markedly increases towards south in our study area (Rosenau 2004) pointing to a southward increasing general dominance of glacial compared to fluvial erosion. Glacial erosion by warm-based glaciers, characteristic for mid-latitudes, is known to be extremely efficient in erosional mass removal (Burbank 2002, and references therein). It thus provides an explanation for the rapid exhumation close to the continental divide in the southern part of the study area. Further, the area is located in a transition zone with respect to the mode of glaciation during the Pleistocene glacial maxima. South of about 40°S massive icecaps formed which, south of 42°S, reached the Pacific ocean (Bangs & Cande 1997; Andersen et al. 1999). North of 40°S only alpine-type valley glaciers developed (Rabassa & Clapperton 1990) which also were very sensitive to slight warming (Hulton et al. 2002) and thus probably existed for much shorter time spans than glaciation further south. Higher precipitation rates towards the south may also have caused a higher ice flux and thus even more pronounced erosion towards the south. Episodic glaciation was initiated at around 7 Ma in southern South America, with possibly 40 glaciations since (Mercer & Sutter 1982; Rabassa & Clapperton 1990). The duration of episodic glaciation and related erosion is thus consistent with the late Miocene to Recent exhumation documented both by Seifert et al. (2005) and by the new AFT data. We therefore suggest that the AFT exhumation pattern mainly reflects differential, mainly glacial erosion in late Miocene to Recent time. Erosion is identified as the principal agent of exhumation in the area.

Summary and Conclusions

Zircon and apatite fission track data have been used to constrain both the exhumation history and to detect transient thermal anomalies. Several new aspects of the thermal and exhumation history are revealed which have major implications for the understanding of the tectonic,

magmatic, and geomorphic evolution of the South-Central Chilean active continental margin. In the Coastal Cordillera, the zircon fission track history goes back into the Triassic, and apatite fission track data constrain regionally consistent slow exhumation since the Late Cretaceous. In contrast, apatite data from the Andean Main Cordillera document Neogene to Recent exhumation gradients, with very rapid exhumation south of 39°S. The following main conclusions can be drawn:

1) Zircon fission track data indicate that the entire studied Coastal Cordillera segment cooled to below 220-200°C at around 200 Ma, suggesting that, after termination of basal accretion in the southern parts of the Western Series, the Coastal Cordillera region experienced uniform cooling and behaved as a homogeneous and coherent tectonic unit within the active margin 'puzzle'. Any post-Triassic exhumation gradients are below the detection limit of the ZFT method.
2) The last major increments of differential exhumation across the Lanalhue Fault Zone are pre-Late Triassic in age.
3) The Chaihuín granodiorite and related small granitoid bodies in the Valdivia area (39°45'S) are not a local peculiarity but reflect a major magmatic and thermal event which apparently affected large parts of the Coastal Cordillera, at least between 39°S and Chiloé (42°20°S).
4) The Coastal Cordillera tectonic unit experienced fairly uniform slow cooling through the apatite PAZ in Late Cretaceous times. Late Cretaceous and Cenozoic, magmatism-related thermal anomalies locally govern AFT ages.
5) Exhumation has overall been remarkably slow in the Coastal Cordillera, with long-term average rates of 0.03-0.04 mm/a since the Late Triassic (Fig. 6). Cenozoic episodic subsidence and uplift had low amplitudes, and did not result in exhumation events detectable by the apatite fission track method. In the outer Andean forearc no large-scale, long-term, Cenozoic accretion, trench-parallel tilting, faulting, or tectonic erosion processes occurred. The only exception appears to be a major Pliocene to Recent episode of uplift and erosion in the high-relief Cordillera Nahuelbuta segment of the Coastal Cordillera, between 37°S and 38°S (Fig. 6).
6) In the western flank of the Andean Main Cordillera south of 39°S, a Miocene to Recent exhumation gradient is developed, reflecting considerably more rapid exhumation in the internal parts of the orogen towards the continental divide (Fig. 6). This gradient appears to continue across the Liquiñe-Ofqui Fault Zone, indicating that no resolvable Pliocene to Recent differential exhumation occurred at the fault, and that the fault in the study area is not accompanied by a Plio-Pleistocene regional near-surface thermal anomaly.

7) A remarkably steep gradient in Miocene-Pliocene to Recent exhumation rates is documented by the FT data along the axis of the Andes, in the region between 38°and 40°S (Fig. 6). Long-term average Pliocene to Recent exhumation near Liquiñe (39°45'S) is, with rates between 1 and 2 mm/a, almost one order of magnitude more rapid than average Paleogene to Recent exhumation near Lonquimay (38°30'S) and further north. This exhumation gradient correlates with climatic gradients and appears to be causally linked with the intensity of late Miocene to Pleistocene glacial erosion.

Acknowledgements

We thank J. Herwig, G. Arnold, V. Kuntz and M. Dziggel for their help with sample preparation and figure drawing, E. Sobel for critically reading an earlier version of the manuscript, D. Melnick and W. Seifert for discussion and for promoting fieldwork, and all colleagues from the Concepción geoscience community and the Berlin-Potsdam SFB 267 group who supported this work by various means. Careful and constructive reviews by M. Brix and M. Brandon are gratefully acknowledged.

References

Adriasola A (2003) Low temperature thermal history and denudation along the Liquiñe-Ofqui Fault Zone in the Southern Chilean Andes, 41-42°S. Dissertation, Ruhr-Universität Bochum, pp 1-119

Adriasola AC, Thomson SN, Brix MR, Hervé F, Stöckhert B (2006) Postmagmatic cooling and late Cenozoic denudation of the North Patagonian Batholith in the Los Lagos region of Chile, 41°-42°15'S. International Journal of Earth Sciences (Geologische Rundschau) 95:504-528

Adriasola A, Stöckhert B, Hervé F (2002) Low temperature thermochronology and tectonics in the Chiloé region, Southern Chilean Andes (41°-43°S; 72°-74°W). 5th International Symposium on Andean Geodynamics, Toulouse 2002, Abstract volume, pp 15-18

Aguirre Le-Bert L, Hervé F, Godoy E (1972) Distribution of metamorphic facies in Chile - An outline. Krystalinikum 9:7-19

Andersen B, Denton GH, Lowell TV (1999) Glacial Geomorphologic Maps of Llanquihue Drift in the Area of the Southern Lake District, Chile. Geografiska Annaler, Series A (Physical Geography) 81/2:155-166

Angermann D, Klotz J, Reigber C (1999) Space-geodetic estimation of the Nazca-South America Euler vector. Earth and Planetary Science Letters 171:329-334

Bangs NL, Cande SC (1997) Episodic development of a convergent margin inferred from structures and processes along the southern Chile margin. Tectonics 16:489-503

Belmar M, Schmidt STh, Ferreiro Mählmann R, Mullis J, Stern WB, Frey M (2002) Diagenesis to low-grade burial and contact metamorphism in the Triassic-Jurassic of the Vichuquén-Tilicura and Hualañe Gualleco Basins, Coastal Range of Chile. Schweizerische Mineralogische und Petrographische Mitteilungen 82/2:375-392

Bernet M, Brandon MT, Garver J, Reiners P, Fitzgerald P (2002) Determining the zircon fission track closure temperature. Geological Society of America, Abstracts with Programs, 34/5:66

Bonnet S, Crave A (2003) Landscape response to climate change: Insights from experimental modeling and implications for tectonic versus climatic uplift of topography. Geology 31:123-126

Brandon MT, Roden-Tice MK, Garver JI (1998) Late Cenozoic exhumation of the Cascadia accretionary wedge in the Olympic mountains, northwest Washington State. Geological Society of America, Bulletin 110:985-1009

Burbank DW (2002) Rates of erosion and their implications for exhumation. Mineralogical Magazine 66:25-52

Cembrano J, Hervé F, Lavenu A (1996) The Liquiñe-Ofqui Fault Zone: a long lived intra arc fault system in southern Chile. Tectonophysics 259:55-66

Cembrano J, Lavenu A, Reynolds P, Arancibia G, López G, Sanhueza A (2002) Late Cenozoic transpressional ductile deformation north of the Nazca-South America-Antarctica triple junction. Tectonophysics 354:289-314

Charrier R (1979) El Triásico en Chile y regiones adyacentes de Argentina: una reconstrucción paleogeografica y paleoclimatica. Comunicaciones, Universidad de Chile, Departamento de Geología, No 26, Santiago de Chile, pp 1-37

Clauser C, Huenges E (1995) Thermal conductivity of rocks and minerals. In: Rock Physics and Phase Relations. A Handbook of Physical Constants, American Geophysical Union Reference Shelf 3:105-126

Collao S, Glodny J, Bascuñán S, Esparza E, Pérez S, Aguilar G (2003) Microtermometría y Cronología en cuarzo de estructuras post-Carbonífero en el basamento metamórfico de Chile Centro-Sur. X. Congreso Geologico Chileno, Concepción 2003, Electronic Abstract Volume, 11 pp

Duhart P, McDonough M, Muñoz J, Martin M, Villeneuve M (2001) El Complejo Metamórfico Bahía Mansa en la cordillera de la Costa del centro-sur de Chile (39°30'-42°00'S): geocronología K-Ar, $^{40}Ar/^{39}Ar$ y U-Pb y implicancias en la evolución del margen sur-occidental de Gondwana. Revista Geológica de Chile 28:179-208

Dumitru TA (1989) Constraints on uplift in the Franciscan subduction complex from apatite fission track analysis. Tectonics 8:197-220

Dumitru TA (1993) A new computer-automated microscope stage system for fission-track analysis. Nuclear Tracks and Radiation Measurements 21:575-580

Emparan C, Suárez M, Muñoz J (1992) Hoja Curacautín, Regiones de la Araucania y del Biobio. Mapa, escala 1:250.000. Carta Geológica de Chile, No. 71, SERNAGEOMIN, Santiago de Chile

Fitzgerald PG, Sorkhabi RB, Redfield TF, Stump E (1995) Uplift and denudation of the central Alaska Range; a case study in the use of apatite fission track thermochronology to determine absolute uplift parameters. Journal of Geophysical Research 100:20175-20191

Franzese JR, Spalletti LA (2001) Late Triassic-early Jurassic continental extension in southwestern Gondwana: tectonic segmentation and pre-break-up rifting. Journal of South American Earth Sciences 14:257-270

Galbraith RF (1981) On statistical models for fission track counts. Journal of Mathematical Geology 13:471-478

Galbraith RF, Laslett GM (1993) Statistical models for mixed fission track ages. Nuclear Tracks and Radiation Measurements 21:459-470

Gallagher K, Brown R, Johnson C (1998) Fission track analysis and its applications to geological problems. Annual Reviews in Earth and Planetary Sciences 26:519-572

Gleadow AJW, Duddy IR, Green PF, Lovering JF (1986) Confined track lengths in apatite - a diagnostic tool for thermal history analysis. Contributions to Mineralogy and Petrology 94:405-415

Glodny J, Lohrmann J, Seifert W, Gräfe K, Echtler H, Figueroa O (2002) Geochronological constraints on material cycling velocities, structural evolution, and exhumation of a paleo-

accretionary wedge: the Bahía Mansa Complex, South Central Chile. 5th International Symposium on Andean Geodynamics, Toulouse, Abstract volume, pp 259-262

Glodny J, Lohrmann J, Echtler H, Gräfe K, Seifert W, Collao S, Figueroa O (2005) Internal dynamics of a paleoaccretionary wedge: insights from combined isotope tectonochronology and sandbox modeling of the South-Central Chilean forearc. Earth and Planetary Science Letters 231:23-39

Glodny J, Echtler H, Figueroa O, Franz G, Gräfe K, Kemnitz H, Kramer W, Krawczyk C, Lohrmann J, Lucassen F, Melnick D, Rosenau M, Seifert W (2006) Long-term geological evolution and mass flow balance of the South-Central Andes. In: Oncken O, Chong G, Franz G, Giese P, Götze HJ, Ramos V, Strecker M, Wigger P (eds): The Andes – Active Subduction Orogeny. Frontiers in Earth Sciences, Vol. 1, Springer Verlag (in press)

Gräfe K, Frisch W, Villa IM, Meschede M (2002) Geodynamic evolution of southern Costa Rica related to low-angle subduction of the Cocos Ridge: constraints from thermochronology. Tectonophysics 348:187-204

Green PF, Duddy IR, Gleadow AJW, Lovering JF (1989) Apatite fission-track analysis as a paleotemperature indicator for hydrocarbon exploration. In: Naeser ND, McCulloh TH (eds). Thermal history of Sedimentary Basins: Methods and Case Histories. Springer, New York, pp 181-195

Hamza VM, Muñoz M (1996) Heat flow map of South America. Geothermics 25:599-646

Hervé M (1976) Estudio geológico de la falla Liquiñe-Reloncaví en el área de Liquiñe; antecedentes de un movimiento transcurrente (Provincia de Valdivia). Congreso Geológico Chileno, Santiago, 1:B39-B56.

Hervé F, Thiele R, Parada MA (1976) Observaciones geológicas en el Triásico de Chile central entre las latitudes 35°30' y 40°00' sur. Congreso Geológico Chileno, Santiago, 1:A297-313

Hervé F, Munizaga F, Parada MA, Brook M, Pankhurst RJ, Snelling NJ, Drake R (1988) Granitoids of the Coast Range of central Chile: Geochronology and geologic setting. Journal of South American Earth Sciences 1:185-194

Hulton NRJ, Purves RS, McCulloch RD, Sugden DE, Bentley MJ (2002) The Last Glacial Maximum and deglaciation in southern South America. Quaternary Science Reviews 21:233-241

Hurford AJ (1990) Standardization of fission track dating calibration: recommendation by the Fission Track Working Group of the I.U.G.S Subcommission on Geochronology. Chemical Geology 80:171-178

Jordan TE, Burns WM, Veiga R, Pángaro F, Copeland P, Kelley S, Mpodozis C (2001) Extension and basin formation in the southern Andes caused by increased convergence rate: A mid-Cenozoic trigger for the Andes. Tectonics 20:308-324

Kamp, PJJ (1999) Tracking crustal processes by FT thermochronology in a forearc high (Hikurangi margin, New Zealand) involving Cretaceous subduction termination and mid-Cenozoic subduction initiation. Tectonophysics 307:313-343

Kemnitz H, Kramer W, Rosenau M (2005) Jurassic to Tertiary tectonic, volcanic, and sedimentary evolution of the Southern Andean intra-arc zone, Chile (38°S-39°S) a survey. Neues Jahrbuch für Geologie und Paläontologie, Abhandlungen 236:19-42

Ketcham RA, Donelick RA, Donelick MB (2000) AFTSolve: A program for multi-kinetic modeling of apatite fission-track data. Geological Materials Research 2/1 (electronic)

Ketcham RA, Donelick RA (2003) AFTSolve, version 1.3.0., Program and documentation. Donelick Analytical Inc. & R.A. Ketcham

Lara L, Moreno H (1998) Geología preliminar area de Liquiñe-Neltume, Región de Los Lagos. Mapa 13, escala 1:100.000. In: SERNAGEOMIN (1998) Estudio Geológico-Económico de la X Región Norte, Informe Registrado IR-98-15, Santiago de Chile

Le Roux JP, Elgueta S (2000) Sedimentologic development of a late Oligocene-Miocene forearc embayment, Valdivia Basin Complex, southern Chile. Sedimentary Geology 130:27-44

Lucassen F, Trumbull R, Franz G, Creixell C, Vásquez P, Romer RL, Figueroa O (2004) Distinguishing crustal recycling and juvenile additions at active continental margins: the Paleozoic to recent compositional evolution of the Chilean Pacific margin (36°-41°S). Journal of South American Earth Sciences 17:103-119

Martin MW, Kato TT, Rodriguez C, Godoy E, Duhart P, McDonough M, Campos A (1999) Evolution of the late Paleozoic accretionary complex and overlying forearc-magmatic arc, south central Chile (38°-41°S): Constraints for the tectonic setting along the southwestern margin of Gondwana. Tectonics 18:582-605

Mas L, Mas G, Bengochea L (2000) Heat flow of Copahue geothermal field, its relation with tectonic scheme. World Geothermal Congress 2000, Proceedings, Kyushu - Tohoku, Japan, Abstract volume, pp 1419-1424

Melnick D, Echtler H (2006a) Inversion of forearc basins in south-central Chile caused by rapid glacial age trench fill. Geology (in press)

Melnick D, Echtler H (2006b) Morphotectonic and geologic digital map compilations of the south-central Andes (36°-42°S). In: Oncken O, Chong G, Franz G, Giese P, Götze HJ, Ramos V, Strecker M, Wigger P (eds.) The Andes - Active Subduction Orogeny. Frontiers in Earth Sciences, Vol. 1, Springer, Berlin, Heidelberg (in press)

Melnick D, Rosenau M, Folguera A, Echtler HP (2006a) Neogene tectonic evolution of the Neuquén Andes western flank (37-39°S), in Kay, S.M., and Ramos, V.A., eds., Evolution of an Andean margin: A tectonic and magmatic view from the Andes to the Neuquén Basin (35°-39°S lat), Geological Society of America Special Paper 407:73-95; doi: 10.1130/2006.2407(04)

Melnick D, Bookhagen B, Echtler HP, Strecker MR (2006b) Coastal deformation and great subduction earthquakes, Isla Santa María, Chile (37°S), Geological Society of America Bulletin 118, doi:10.1130/B25865.1 (in press)

Mercer JH, Sutter JF (1982) Late Miocene-earliest Pliocene glaciation in southern Argentina. Palaeogeography, Palaeoclimatology, Palaeoecology 38:185-206

Moore MA, England PC (2001) On the inference of denudation rates from cooling ages of minerals. Earth and Planetary Science Letters 185:265-284

Mordojovich C (1981) Sedimentary basins of Chilean Pacific offshore. In: Halbouty MT (ed.) Energy resources of the Pacific region. American Association of Petroleum Geologists, Studies in Geology 12, pp 63-82

Mpodozis C, Ramos V (1989) The Andes of Chile and Argentina. In: Ericksen GE, Cañas Pinochet MT, Reinemund JA (eds) Geology of the Andes and its Relation to Hydrocarbon and Mineral Resources. Circum-Pacific Council for Energy and Mineral Resources Earth Science Series, Vol. 11, Houston, Texas, pp 59-90

Muñoz J, Troncoso R, Duhart P, Crignola P, Farmer L, Stern CR (2000) The relation of the mid-Tertiary coastal magmatic belt in south-central Chile to the late Oligocene increase in plate convergence rate. Revista Geológica de Chile 27:177-203

Nelson ST, Davidson JP, Heizler MT, Kowallis BJ (1999) Tertiary tectonic history of the southern Andes: The subvolcanic sequence to the Tatara-San Pedro volcanic complex, lat 36°S. Geological Society of America, Bulletin 111:1387-1404

New MG, Hulme M, Jones PD (1999) Representing 20th century space-time climate variability. I: Development of a 1961-1990 mean monthly terrestrial climatology. Journal of Climate 12:829-856

New MG, Lister D, Hulme M, Makin I (2002) A high-resolution data set of surface climate over global land areas. Climate Research 21:1-25

Pankhurst RJ, Hervé F, Rojas L, Cembrano J (1992) Magmatism and tectonics in continental Chiloé, Chile (42°-42°30'S). Tectonophysics 205:283-294

Platt JP, England PC (1993) Convective removal of lithosphere beneath mountain belts: thermal and mechanical consequences. American Journal of Science 294:307-336

Potent S (2003) Kinematik und Dynamik neogener Deformationsprozesse des südzentralchilenischen Subduktionssystems, nördlichste Patagonische Anden (37°-40°S). Doctoral thesis, Univ. Hamburg, pp 1-169

Rabassa J, Clapperton CM (1990) Quaternary glaciations of the Southern Andes. Quaternary Science Reviews 9:153-174

Rahn MK, Brandon MT, Batt GE, Garver JI (2004) A zero-damage model for fission-track annealing in zircon. American Mineralogist 89:473–484

Rauch K (2005) Cyclicity of Peru-Chile trench sediments between 36° and 38°S: A footprint of paleoclimatic variations?. Geophysical Research Letters 32:L08302, doi: 10.1029/2004GL022196

Rehak K (2005) Morphometrische Analyse eines aktiven Kontinentalrandes - Cordillera de Nahuelbuta (Chile). Geographisches Institut der Humboldt-Universität zu Berlin, Arbeitsberichte, Heft 107, ISSN 0947-0360, Berlin

Reiners P, Brandon M (2006) Using thermochronology to understand orogenic erosion. Annual Reviews of Earth and Planetary Sciences 34:419-466.

Ring U, Brandon MT, Willett SD, Lister GS (1999) Exhumation processes. In: Ring U, Brandon MT, Lister GS, Willett SD (eds.) Exhumation processes: Normal faulting, ductile flow and erosion, Geological Society, London, Special Publication 154, pp 1-27

Rosenau MR (2004) Tectonics of the Southern Andean Intra-arc Zone (38° - 42°S). Dissertation, Freie Universität Berlin, http://www.diss.fu-berlin.de/2004/280/index.html, pp 1-154

Rosenau M, Melnick D, Echtler H (2006) Kinematic constraints on intra-arc shear and strain partitioning in the southern Andes between 38°S and 42°S latitude. Tectonics 25, doi: 10.1029/2005TC001943 (in press)

Rothstein DA, Manning CE (2003) Geothermal gradients in continental magmatic arcs: Constraints from the eastern Peninsular Ranges batholith, Baja California, México. Geological Society of America, Special Paper 374:337-354

Rutland RWR (1971) Andean orogeny and sea floor spreading. Nature 233:252-255

Seifert W, Rosenau M, Echtler H (2005) Crystallization depths of granitoids of South Central Chile estimated by Al-in-hornblende geobarometry: implications for mass transfer processes along the active continental margin. Neues Jahrbuch für Geologie und Paläontologie, Abhandlungen 236:115-127

Seipold U (1998) Temperature dependence of thermal transport properties of crystalline rocks - A general law. Tectonophysics 291:161-171

SERNAGEOMIN (2003). Mapa Geológico de Chile: versión digital. Servicio Nacional de Geología y Minería, Publicación Geológica Digital, No. 4 (CD-ROM, versión 1.0, 2003), Santiago de Chile

Smith WHF, Sandwell DT (1997) Global Seafloor Topography from Satellite Altimetry and Ship Depth Soundings. Science 277:1956-1962

Spotila JA, Buscher JT, Meigs AJ, Reiners PW (2004) Long-term glacial erosion of active mountain belts: Example of the Chugach-St. Elias Range, Alaska. Geology 32:501-504

Stüwe K, White L, Brown R (1994) The influence of eroding topography on steady-state isotherms. Application to fission track analysis. Earth and Planetary Science Letters 124:63-74

Suárez M, Emparan C (1995) The stratigraphy, geochronology and paleophysiography of a Miocene fresh-water interarc basin, southern Chile. Journal of South American Earth Sciences 8:17-31

Tagami T, Galbraith RF, Yamada R, Laslett GM (1998) Revised annealing kinetics of fission tracks in zircon and geological implications. In: Van Den Haute P, De Corte F (eds.) Advances in Fission-Track Geochronology, Kluwer, Dordrecht, pp 99-112

Thomson SN (2002) Late Cenozoic geomorphic and tectonic evolution of the Patagonian Andes between latitudes 42° and 46°S: An appraisal based on fission-track results from the

transpressional intra-arc Liquiñe-Ofqui fault zone. Geological Society of America, Bulletin, 114:1159-1173

Thomson SN, Hervé F (2002) New time constraints for the age of metamorphism at the ancestral Pacific Gondwana margin of southern Chile (42-52°S). Revista Geológica de Chile 29:151-165

Vietor T, Echtler H (2006) Episodic Neogene southward growth of the Andean subduction orogen between 30°S and 40°S - plate motions, mantle flow, climate, and upper-plate structure. In: Oncken O, Chong G, Franz G, Giese P, Götze HJ, Ramos V, Strecker M, Wigger P (eds): The Andes - Active Subduction Orogeny. Frontiers in Earth Sciences, Vol. 1, Springer, Berlin, Heidelberg (in press).

Von Huene R, Ranero CR (2003) Subduction erosion and basal friction along the sediment-starved convergent margin off Antofagasta, Chile. Journal of Geophysical Research 108, B2, 2079, DOI:10.1029/2001JB001569

Wagner GA (1979) Correction and interpretation of fission track ages. In: Jäger E, Hunziker J (eds) Lectures in Isotope Geology. Springer, Berlin, pp 170-177

Waite K, Fügenschuh B, Schmidt S, Schmid S (2005) A fission track study on low-grade metamorphism and stratigraphy in the Central Chilean Andes. 19th Colloquium on Latin American Geosciences – Potsdam, Germany. Terra Nostra 05/1: 137

Willett SD (1999) Orogeny and orography: The effects of erosion on the structure of mountain belts. Journal of Geophysical Research 104(B12):28957-28981

Willett SD, Fisher D, Fuller C, En-Chao Y, Chia-Yu L (2003) Erosion rates and orogenic wedge kinematics in Taiwan inferred from fission-track thermochronometry. Geology 31:945-948

Willner AP, Hervé F, Massonne HJ (2000) Mineral chemistry and pressure-temperature evolution of two contrasting high-pressure-low-temperature belts in the Chonos archipelago, Southern Chile. Journal of Petrology 41:309-330

Willner AP, Pawlig S, Massonne HJ, Hervé F (2001) Metamorphic evolution of spessartine quartzites (Coticules) in the high-pressure, low temperature complex at Bahía Mansa, Coastal Cordillera of South-Central Chile. Canadian Mineralogist 39:1547-1569

Willner AP (2005) Pressure–Temperature Evolution of a Late Palaeozoic Paired Metamorphic Belt in North–Central Chile (34°–35°30' S). Journal of Petrology 46:1805-1833

Willner AP, Thomson S, Kröner A, Wartho JA, Wijbrans JR, Hervé F (2005) Time markers for the evolution and exhumation history of a Late Paleozoic paired metamorphic belt in north-central Chile (34-35°30'S). Journal of Petrology, DOI:10.1093/petrology/egi036

Figures

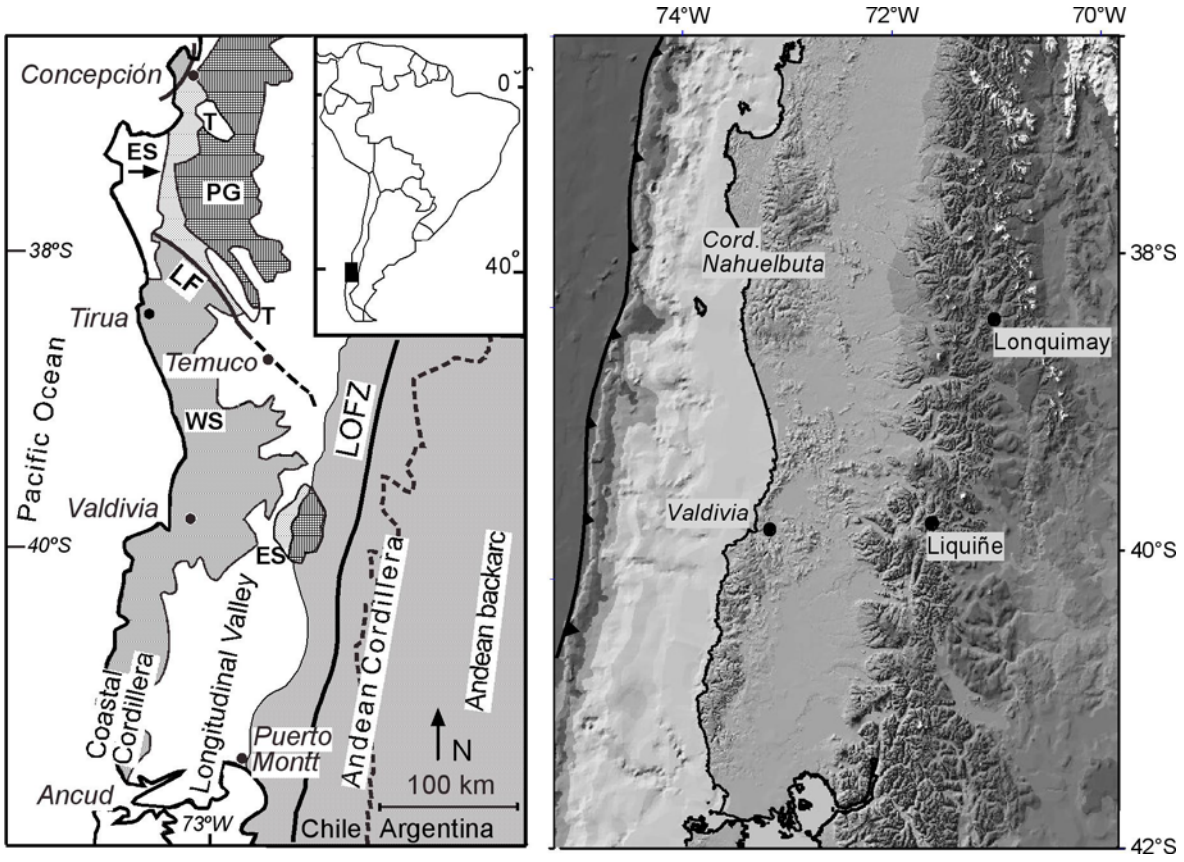

Fig. 1. Geologic sketch map of South-Central Chile, with morphotectonic units. WS - Western Series palaeoaccretionary complex; ES, Eastern Series; PG, late Palaeozoic granitoids; T, Triassic sediments; LF, Lanalhue Fault Zone; LOFZ, Liquiñe-Ofqui Fault Zone. For comparison: Digital elevation model, compiled with TOPEX (Smith & Sandwell 1997) and SRTM data.

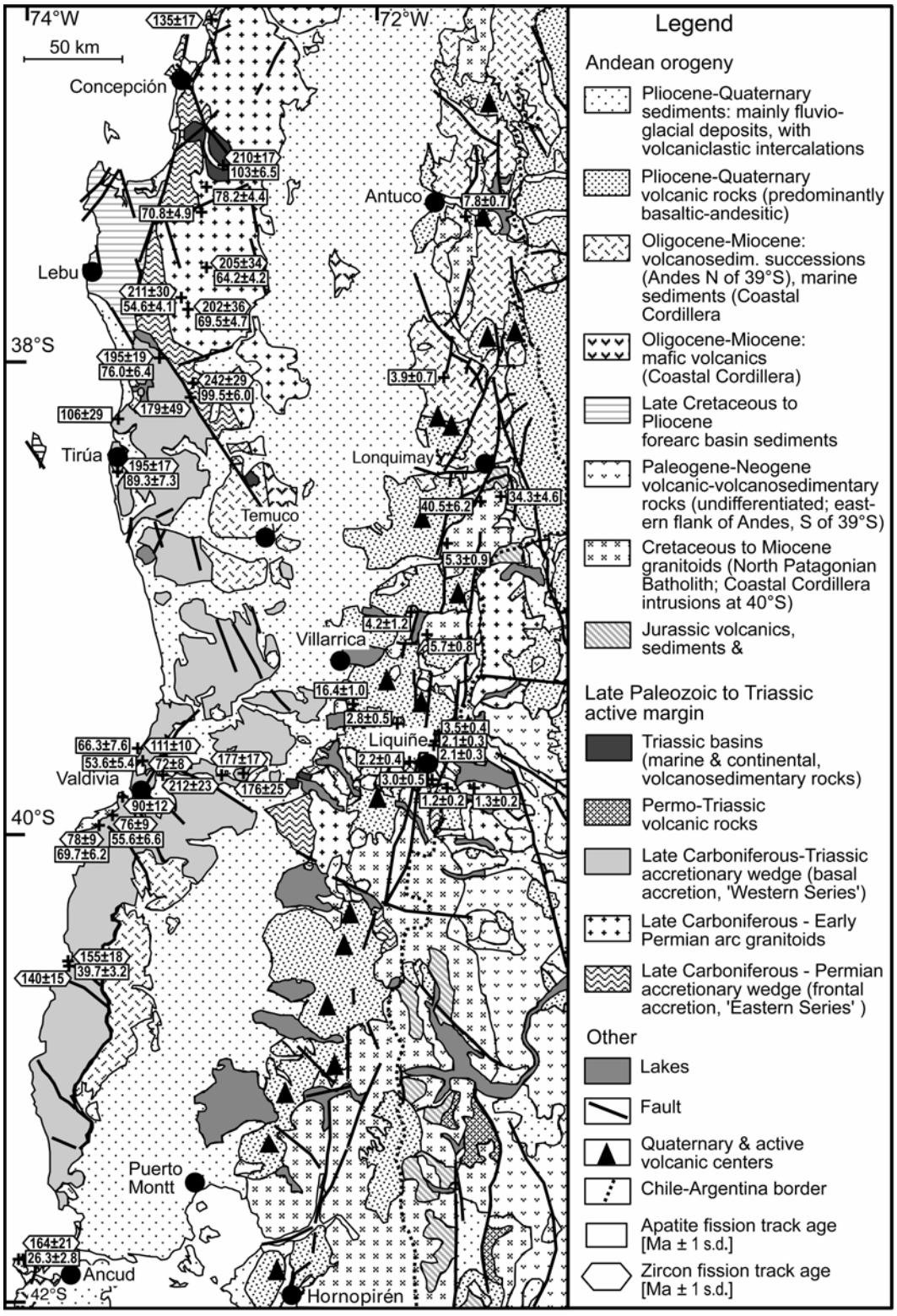

Fig. 2. Geologic map of South-Central Chile and adjacent parts of Argentina (modified after SERNAGEOMIN 2003, Melnick and Echtler 2006b), between 36°30' S and 42°S, with results and locations of fission track analyses discussed in this study.

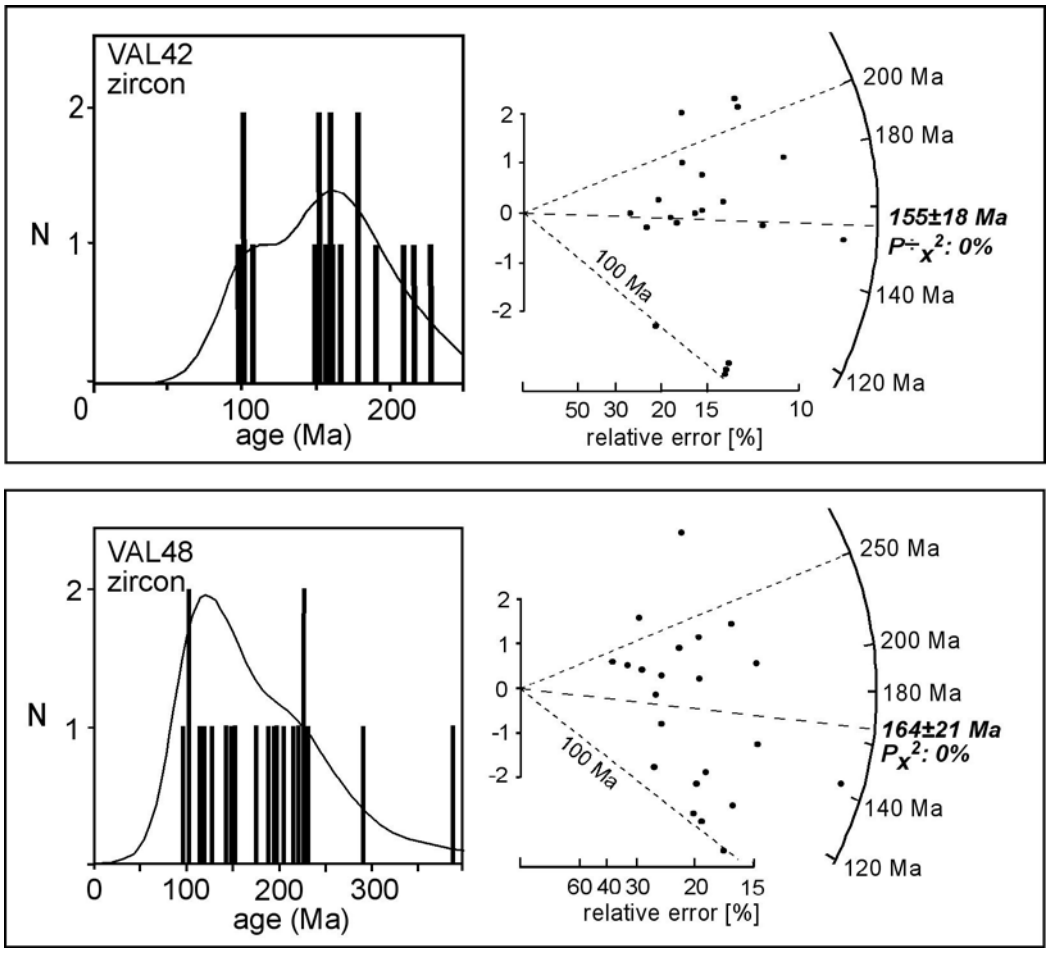

Fig. 3. Zircon fission track single grain age data, as age histograms and radial plots, for samples VAL42 and VAL48, Coastal Cordillera south of 40°S. Note large dispersion of individual grain ages, interpreted as due to partial reset of ~200 Ma ages by thermal overprint at 90-100 Ma.

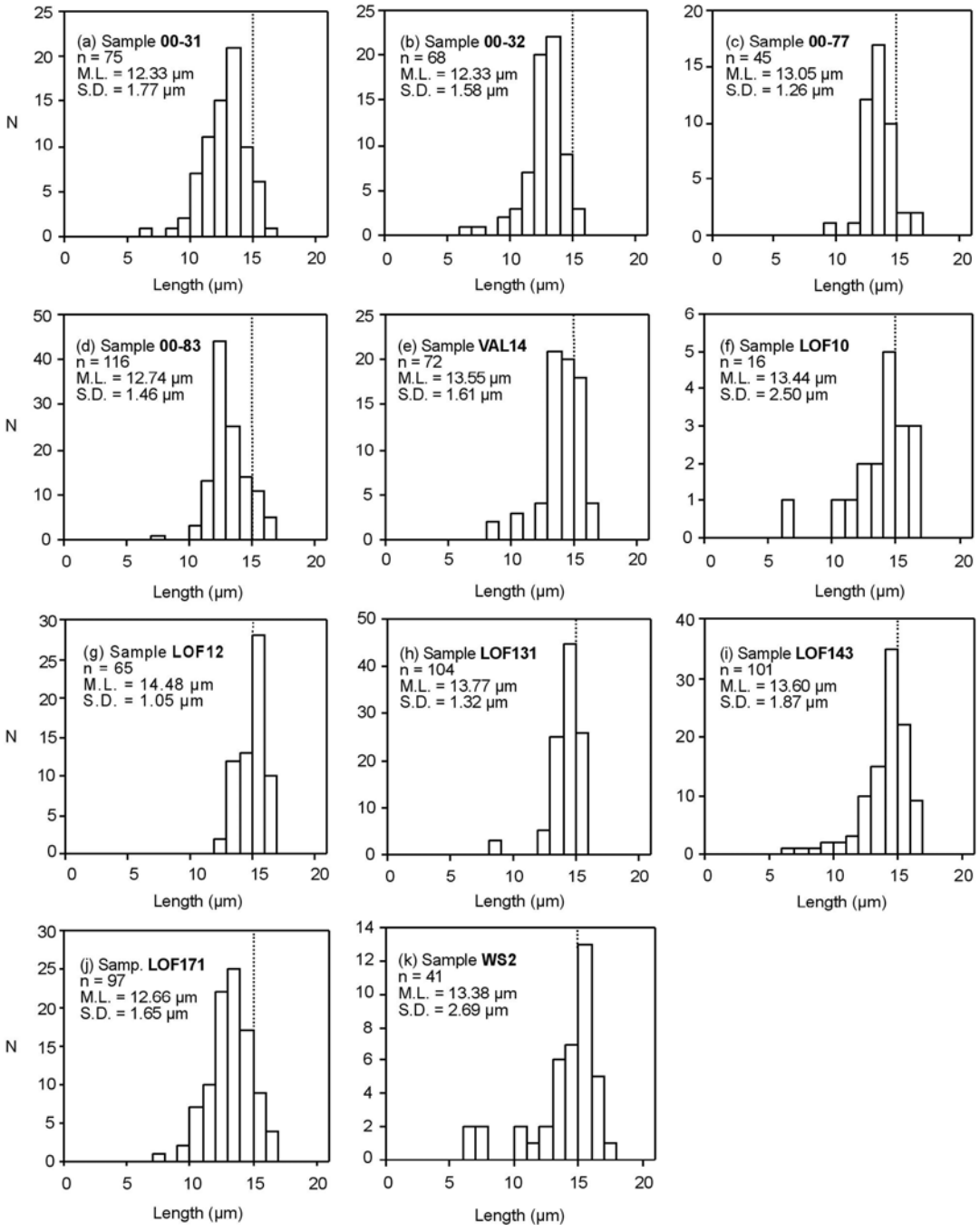

Fig. 4. Fission track length distribution diagrams for apatite samples. Samples (a)-(e) are from the Coastal area and Coastal Cordillera; (f)-(k) are from the Andes. N (number of tracks) plotted versus track length (microns). n, total number of tracks counted; M.L., mean track length; S.D., standard deviation. Stippled lines at 15 µm as an aid for orientation.

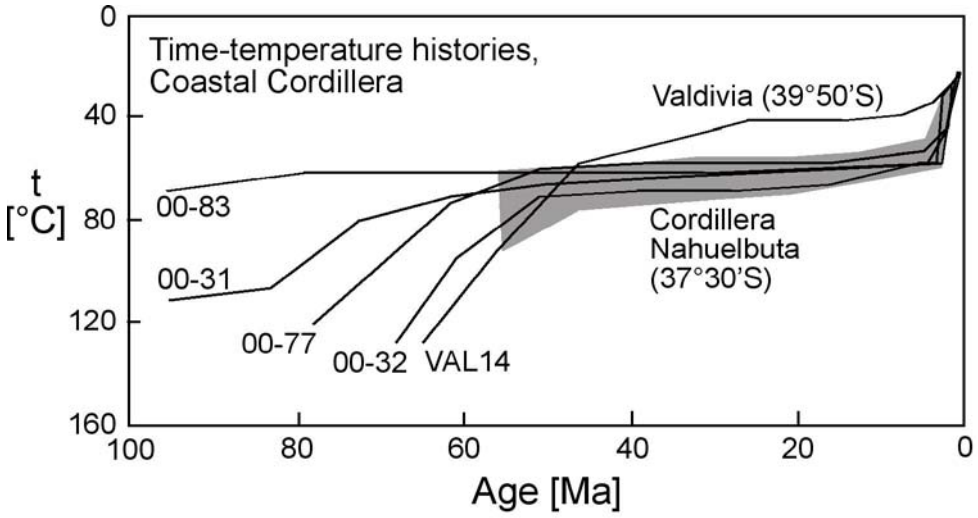

Fig. 5. Results of inverse modelling of apatite fission track length data (see Fig. 4), Coastal Cordillera of South-Central Chile. Shaded field denotes the range of good-fit results for samples from the high-relief parts of the Cordillera Nahuelbuta.

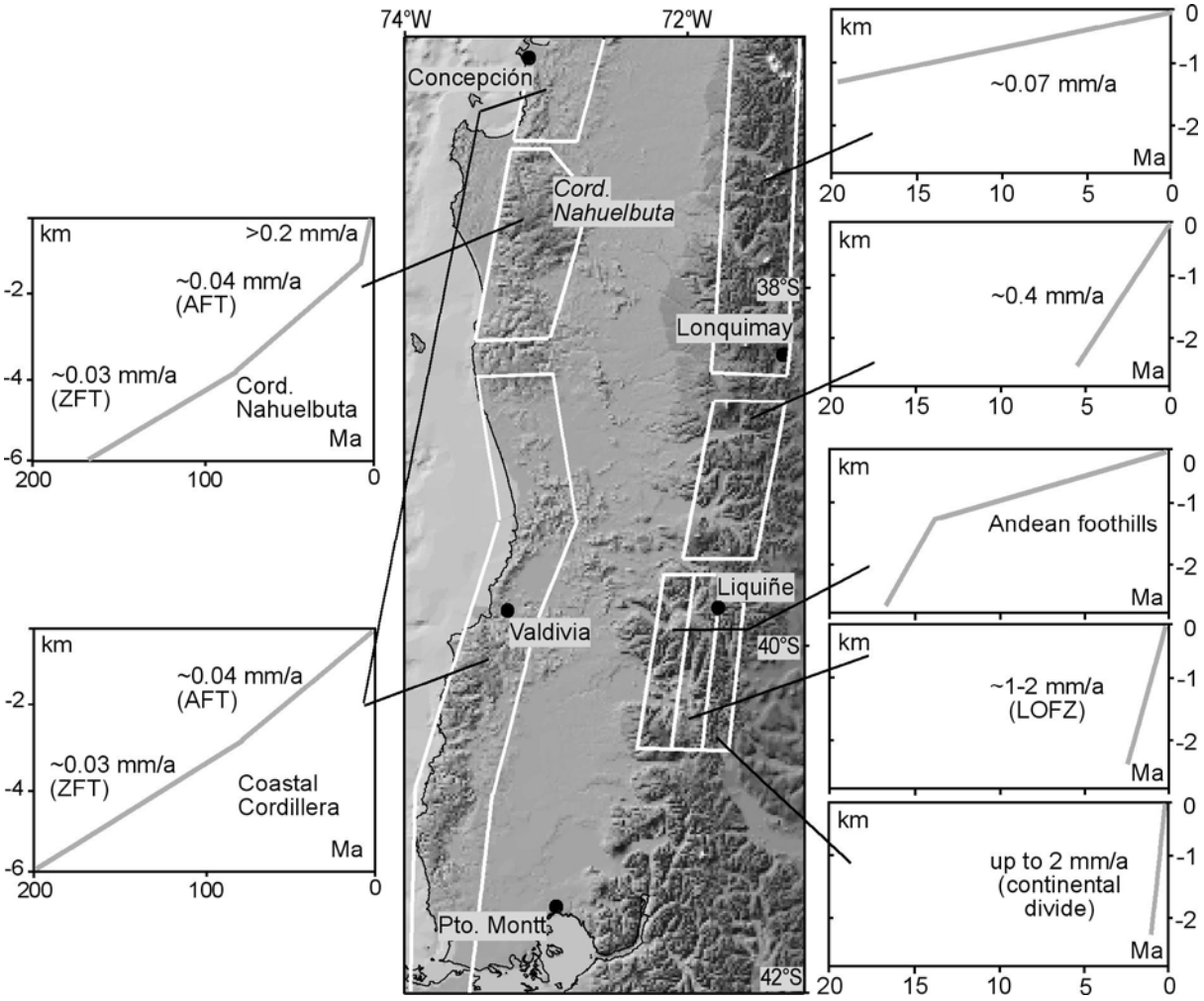

Fig. 6. Schematic summary of the exhumation rate results for the South-Central Chilean continental margin, based on zircon fission track (ZFT) and apatite fission track (AFT) data. LOFZ: Liquiñe-Ofqui Fault Zone area near Liquiñe, roughly 20 km west of the Andean continental divide. See text for discussion.

Tables

Table 1. Apatite and zircon standard data

Analysis #	Dosimeter glass	standard material used	No. grains	ρ_s x 10^5 [cm^{-2}]	N_s	ρ_i x 10^5 [cm^{-2}]	N_i	P χ^2 [%]	Age disp. [%]	Zeta value (± 2σ)
ZF-1	CN2	zircon, Fish Canyon Tuff	15	44.7	1924	55.5	2388	0	21	149 ± 10
ZF-2	CN2	zircon, Fish Canyon Tuff	20	50.8	2436	62.1	2977	0.7	12	148 ± 10
ZF-3	CN2	zircon, Fish Canyon Tuff	19	58.5	2435	67.9	2826	7.8	8	140 ± 10
ZF-4	CN2	zircon, Fish Canyon Tuff	15	71.6	2387	78.8	2629	40	3	134 ± 10
AD 2-1	CN5	apatite, Durango	20	1.55	272	10.7	1872	40	10	330 ± 44
AF 1-1	CN5	apatite, Fish Canyon Tuff	20	2.25	238	18.5	1963	80	<1	349 ± 50
DUR-3	CN5	apatite, Durango	15	1.75	181	11.6	1202	64	2	368 ± 60
DUR-K	CN5	apatite, Durango	17	1.47	347	9.58	2256	67	1	360 ± 44
FCT-3	CN5	apatite, Fish Canyon Tuff	20	1.82	235	13.5	1752	92	<1	365 ± 54

Abbreviations: ρ_s and ρ_i, spontaneous and induced track densities in the standards; N_s and N_i, number of spontaneous and induced tracks counted; $P\chi^2$ is the probability of obtaining χ^2 values for υ degrees (υ= number of mineral grains - 1) of freedom; Age disp., age dispersion.

Table 2. Zircon fission track data (Coastal Cordillera, South Central Chile)

Sample	GPS location, altitude [m]	material (age of formation / last metamorphism)	No. grains	ρ_s x 10^5 [cm^{-2}]	N_s	ρ_i x 10^5 [cm^{-2}]	N_i	P χ^2 [%]	Age disp. [%]	[U]	ρ_d x 10^5 [cm^{-2}]	N_d	Age [Ma] ± 1σ
01-27	36°34.99'S 72°58.81'W (10)	sandstone (Cretaceous)	20	146.0	3358	33.91	780	0	40	266	4.54	3000	135 ± 17
01-50	37°10.10'S 72°57.25'W (50)	sandstone (Triassic)	20	203.5	6062	32.27	961	23	6	288	4.75	3000	210 ± 17
00-77	37°37.08'S 73°07.72'W (900)	granite (Late Carboniferous)	4	378.9	305	64.60	52	47	<1	479	4.97	3174	205 ± 34
00-32	37°44.55'S 73°08.23'W (600)	granite (Late Carboniferous)	5	469.6	486	78.26	81	85	<1	546	5.00	3174	211 ± 30
00-31	37°45.44'S 73°09.20'W (600)	granite (Late Carboniferous)	5	420.6	532	77.47	98	5	25	560	5.02	3174	202 ± 36
01-40	38°01.45'S 73°08.22'W (162)	metapsammite (Low. Perm.)	14	184.1	2498	31.02	421	10	14	263	4.66	3000	195 ± 19
01-35	38°09.81'S 72°53.79'W (74)	phyllitic schist (Lower Perm.)	11	199.8	988	26.69	132	29	6	210	4.60	3000	242 ± 29
01-37	38°11.00'S 72°56.55'W (142)	metapsammite (Low. Perm.)	4	117.4	243	36.23	75	2	35	307	4.62	3000	179 ± 49
01-04	38°20.60'S 73°29.20'W (0)	albite schist (Lower Permian)	13	234.7	2969	36.76	465	68	<1	309	4.33	3000	195 ± 17
VAL11	39°40.53'S 73°21.34'W (10)	quartzitic schist (Early Trias.)	18	98.7	1907	30.64	592	7	14	236	4.78	3177	111 ± 10
VAL10	39°41.31'S 73°20.83'W (370)	granitoid (Cretaceous)	20	157.2	5024	76.54	2447	9	7	592	4.80	3177	72 ± 8
VAL25*	39°48.23'S 73°09.10'W (30)	micaschist (Early Triassic)	20	238.0	4024	35.61	602	0	29	308	4.58	3174	212 ± 23
VAL21*	39°48.38'S 72°52.14'W (47)	albite schist (Early Triassic)	20	149.6	2133	28.89	412	0	34	240	4.73	3177	176 ± 25
VAL24*	39°48.42'S 73°02.78'W (50)	mafic schist (Early Triassic)	13	252.1	2319	44.64	411	0.1	22	384	4.59	3174	177 ± 17
VAL19	39°53.37'S 73°26.17'W (60)	quartzitic schist (Early Trias.)	4	298.9	275	109.8	101	63	<1	875	4.66	3174	90 ± 12
VAL14	39°54.18'S 73°29.88'W (30)	granitoid (Cretaceous)	20	147.8	4300	68.57	1995	0	18	530	4.77	3177	76 ± 9
VAL17	39°57.43'S 73°36.05'W (0)	granitoid (Cretaceous)	21	100.8	4779	48.90	2321	0	18	376	4.75	3177	78 ± 9
VAL42	40°35.02'S 73°44.34'W (0)	micaschist (Triassic)	20	216.8	5510	47.37	1204	0	19	388	4.69	3177	155 ± 18
VAL45	40°35.78'S 73°44.13'W (10)	quartzitic schist (Triassic)	17	146.1	3779	35.87	928	23	5	333	4.68	3177	140 ± 15
VAL48	41°48.02'S 74°01.43'W (0)	phyllitic schist (Triassic)	22	161.8	3494	33.44	722	0	29	270	4.67	3177	164 ± 21

Abbreviations: ρ_s and ρ_i, spontaneous and induced track densities in the zircon sample; ρ_d, density of induced tracks in the dosimeter glass; N_s and N_i, number of spontaneous and induced tracks counted; N_d, number of tracks counted in CN2 dosimeter glass; $P\chi^2$ is the probability of obtaining χ^2 values for υ degrees (υ= number of mineral grains - 1) of freedom; Age disp., age dispersion; [U]-uranium concentration (ppm) in sample.. * denotes analyses previously published (Glodny et al. 2005). Fission track ages are reported as central ages (Galbraith & Laslett 1993). Zeta/CN2 = 143 ± 10. Age information on crystallization / metamorphism is from Glodny et al. (2005), Martin et al. (1999), Duhart et al. (2001), and unpublished data by the authors.

Table 3. Apatite fission track data (Coastal Cordillera, South Central Chile)

Sam-ple	GPS location, (altitude [m])	material (age of formation)	No. grs.	ρ_s x 10^5 [cm^{-2}]	N_s	ρ_i x 10^5 [cm^{-2}]	N_i	$P\chi^2$ [%]	Age disp [%]	[U]	ρ_d x10^5 [cm^{-2}]	N_d	Age [Ma] ± 1σ	Mean tr. length [µm ± s.d.] (No. of tracks)
01-50	37°10.10'S 72°57.25'W (50)	sandstone (Tr)	30	19.6	1905	46.02	4473	0	19	40	13.76	9222	103 ± 6.5	
00-83	37°15.43'S 72°57.60'W (200)	diorite (C-P)	20	11.4	1283	35.25	3981	21	5	31	13.80	6483	78.2 ± 4.4	12.74± 1.46 (116)
00-79	37°23.88'S 73°03.54'W (700)	granite (C-P)	20	18.0	1124	61.65	3847	0	18	56	13.70	6483	70.8 ± 4.9	
00-77	37°37.08'S 73°07.72'W (900)	granite (C-P)	13	6.66	529	24.85	1973	78	<1	24	13.60	6483	64.2 ± 4.2	13.05±1.26 (45)
00-32	37°44.55'S 73°08.23'W (600)	granite (C-P)	20	5.94	488	26.03	2136	11	14	25	13.51	6483	54.6 ± 4.1	12.33±1.58 (68)
00-31	37°45.44'S 73°09.20'W (600)	granite (C-P)	20	6.74	725	22.69	2442	9	13	21	13.41	6483	69.5 ± 4.7	12.33±1.77 (75)
01-40	38°01.45'S 73°08.22'W (162)	qtz schist (P)	15	8.91	367	29.41	1211	11	15	30	13.87	9222	76.0 ± 6.4	
01-35	38°09.81'S 72°53.79'W (74)	phyll. schist (P)	29	18.2	1198	44.81	2950	8	12	41	14.10	9222	99.5 ± 6.0	
VAL26	38°13.81'S 73°28.09'W (5)	albite schist (P)	28	0.12	20	0.26	44	83	15	0.3	13.33	6667	106 ± 29	
01-04	38°20.60'S 73°29.20'W (0)	albite schist (P)	20	17.4	669	51.90	2000	0	22	50	14.45	9222	89.3 ± 7.3	
VAL11	39°40.53'S 73°21.34'W (10)	micaschist (Tr)	20	4.92	211	17.37	745	11	23	16	13.70	6667	66.3 ± 7.6	
VAL10	39°41.31'S 73°20.83'W (370)	granitoid (Cret.)	20	3.49	169	14.83	717	44	11	15	12.84	6483	53.6 ± 5.4	13.99±1.82 (37)
VAL14	39°54.18'S 73°29.88'W (30)	granitoid (Cret.)	20	3.69	111	15.21	458	30	13	15	13.03	6483	55.6 ± 6.6	13.55±1.61 (72)
VAL17	39°57.43'S 73°36.05'W (0)	granitoid (Cret.)	14	5.21	274	17.29	909	19	12	16	13.12	6483	69.7 ± 6.2	13.91±1.84 (85)
VAL42	40°35.02'S 73°44.34'W (0)	micaschist (Tr)	20	5.21	393	36.67	2769	11	16	29	15.86	7440	39.7 ± 3.2	
VAL48	41°48.02'S 74°01.43'W (0)	phyll. schist (Tr)	30	1.79	139	18.63	1450	55	16	17	15.47	7440	26.3 ± 2.8	

Abbreviations: ρ_s and ρ_i, spontaneous and induced track densities in the apatite sample; No. grs., number of counted grains; ρ_d, density of induced tracks in the dosimeter glass; N_s and N_i, number of spontaneous and induced tracks counted; N_d, number of tracks counted in CN5 dosimeter glass; $P\chi^2$ is the probability of obtaining χ^2 values for υ degrees (υ= number of mineral grains - 1) of freedom; Age disp, Age dispersion; [U]-uranium concentration (ppm) in sample; s.d., standard deviation. Cret., Cretaceous; C-P, Late Carboniferous to Early Permian; P, Permian; Tr, Triassic. Fission track ages are reported as central ages (Galbraith & Laslett 1993). Zeta/CN5 = 354±15. Age information on rock formation (sedimentation, crystallization, or last metamorphism) is from Martin et al. (1999), Glodny et al. (2005), and unpublished data of the authors.

Table 4. Apatite fission track data (Andes, South Central Chile)

Sample	GPS location, (altitude [m])	material (age)	No. grs.	ρ_s x 10^5 [cm^{-2}]	N_s	ρ_i x 10^5 [cm^{-2}]	N_i	P_χ^2 [%]	Age disp [%]	[U]	ρ_d x 10^5 [cm^{-2}]	N_d	Age [Ma] ± 1σ	Mean tr. length [µm ± s.d.] (No. of tracks)
LOF143	37°22.94'S 71°29.39'W (1000)	dio (Mioc.)	20	2.38	250	87.43	9193	11	15	67	16.16	7674	7.8 ± 0.7	13.60±1.87 (101)
LOF145	38°05.61'S 71°42.49'W (850)	gra (Pal.)	20	0.44	39	31.39	2811	23	24	24	16.01	7674	3.9 ± 0.7	-
LOF171	38°33.21'S 71°16.77'W (1270)	gra (Cret.)	20	1.58	112	12.55	889	4	33	11	15.14	7674	34.3 ± 4.6	12.66±1.65 (97)
LOF149	38°35.76'S 71°26.31'W (1350)	dio (Cret.)	20	2.93	299	20.38	2082	23	12	16	15.93	7674	40.5 ± 6.2	-
WS2	38°45.77'S 71°35.89'W (700)	gra (Mioc.)	25	0.54	41	27.66	2084	70	3	23	15.34	7440	5.3 ± 0.9	13.38±2.69 (41)
LOF135	39°02.66'S 71°48.14'W (370)	gra (Mioc.)	20	0.16	14	8.95	777	56	23	8	12.96	8676	4.2 ± 1.2	-
LOF132	39°10.07'S 71°43.54'W (770)	gra (Mioc.)	6	1.76	61	70.58	2449	35	13	59	12.93	8676	5.7 ± 0.8	-
LOF131	39°29.52'S 72°06.59'W (210)	gra (CP)	30	4.37	582	60.94	8110	61	4	58	12.89	8676	16.4 ± 1.0	13.77±1.32 (104)
LOF130	39°37.62'S 71°54.99'W (290)	gra (Mioc.)	30	0.29	40	23.09	3203	52	9	23	12.86	8676	2.8 ± 0.5	-
LOF10	39°41.83'S 71°54.25'W (300)	gra (Mioc.)	30	0.26	42	23.89	3873	14	38	26	11.51	7658	2.2 ± 0.4	13.44±2.50 (16)
LOF12	39°42.98'S 71°48.15'W (1720)	gra (Cret.)	30	0.99	112	55.78	6303	69	8	64	11.16	7658	3.5 ± 0.4	14.48±1.05 (65)
LOF13	500 m SW of LOF12 (1600)	gra (Cret.)	30	0.38	72	36.81	6988	38	6	39	11.64	7658	2.1 ± 0.3	--
LOF14	1200 m SW of LOF12 (1220)	gra (Cret.)	22	0.71	61	70.39	6029	20	27	77	11.70	7658	2.1 ± 0.3	-
LOF17	39°46.56'S 71°50.09'W (1050)	gra (Mioc.)	31	0.34	43	23.40	2968	99	<1	24	11.83	7658	3.0 ± 0.5	-
LOF 78	39°46.58'S 71°41.74'W (1000)	dio (Cret.)	29	0.19	33	33.44	5886	49	10	34	12.44	7658	1.2 ± 0.2	-
LOF18	39°48.58'S 71°34.94'W (1000)	gra (Cret.)	20	0.37	30	61.05	4962	98	<1	12	11.89	7658	1.3 ± 0.2	-

Abbreviations: ρ_s and ρ_i, spontaneous and induced track densities in the apatite sample; ρ_d, density of induced tracks in the dosimeter glass; N_s and N_i, number of spontaneous and induced tracks counted; N_d, number of tracks counted in CN5 dosimeter glass; $P\chi^2$ is the probability of obtaining χ^2 values for υ degrees (υ= number of mineral grains - 1) of freedom; Age disp, Age dispersion; [U]-uranium concentration (ppm) in sample; s.d., standard deviation; dio, diorite; gra, granite; Mioc., Miocene; Pal., Paleocene; Cret., Cretaceous; CP, Late Carboniferous/Early Permian. Fission track ages are reported as central ages (Galbraith & Laslett 1993). Zeta/ CN5 = 354±15. Age information on igneous rock crystallization or early cooling is from SERNAGEOMIN (2003), Rosenau (2003), Emparan et al. (1992), Lara & Moreno (1998).